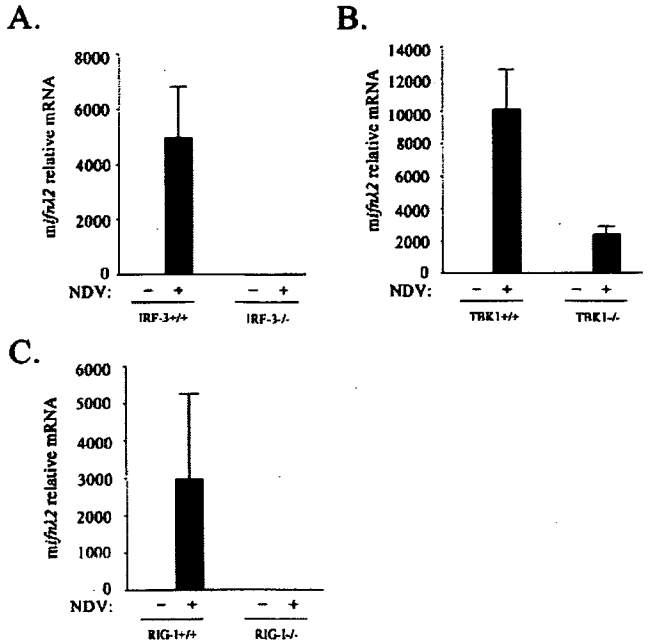

FIGURE 1. **Critical role of IRF-3, TBK1, and RIG-I in NDV-induced activation of the *ifnλ2*.** MEFs derived from mice with wild-type or knocked out IRF-3 (*A*), TBK1 (*B*), and RIG-I (*C*) genes were mock-treated (−) or infected (+) with NDV as indicated. Twelve hours after infection, cells were harvested and mouse *ifnλ2* mRNA levels were determined by quantitative real time-PCR. *Error bars* indicate the S.E. of triplicate measurements.

pair. Thus, comparison is best made between each +/+ and −/−.

Gain of Function of IRF-3 and RIG-I Results in the Activation of Human IFN-λ Genes—As an alternative approach, we expressed dominant active mutants of IRF-3 and RIG-I in 293T cells and monitored endogenous human *ifnλ1* and *ifnλ2* mRNA by quantitative real time-PCR. IRF-3 5D is a mutant with five Ser/Thr residues replaced with Asp. IRF-3 5D is constitutively phosphorylated at Ser-386 by some unknown kinase(s) in human cells and is capable of activating targets including type I IFN genes (17). Overexpression of a deletion mutant of RIG-I, which contains CARD alone (RIG-I CARD, Fig. 2*A*), results in the constitutive activation of type I IFN genes (6). Ectopic expression of constitutively active IRF-3 and RIG-I in 293T cells (Fig. 2*B*) resulted in the constitutive activation of human *ifnλ1* and *ifnλ2* (Fig. 2, *C* and *D*). These results strongly suggest that IFN-λ genes are regulated by a mechanism common to type I IFN.

IFN-λ Genes are Regulated by IPS-1-mediated Signaling—Recently, IPS-1 (also known as MAVS, VISA, or Cardif) was identified as an adaptor molecule of RIG-I signaling (7–10). It has been hypothesized that activated RIG-I interacts with IPS-1 between respective CARD domains, resulting in the activation of IRF-3, NF-κB, and type I IFN genes. Interestingly, overexpression of full-length IPS-1 can induce the expression of type I IFN genes without a viral infection. We therefore expressed full-length IPS-1 in 293T cells (Fig. 2*B*) and monitored human *ifnλ1* and *ifnλ2* mRNA. Transfection of the IPS-1-encoding vector but not empty vector induced the expression of endogenous human *ifnλ1* and *ifnλ2* (Fig. 2, *E* and *F*), suggesting that

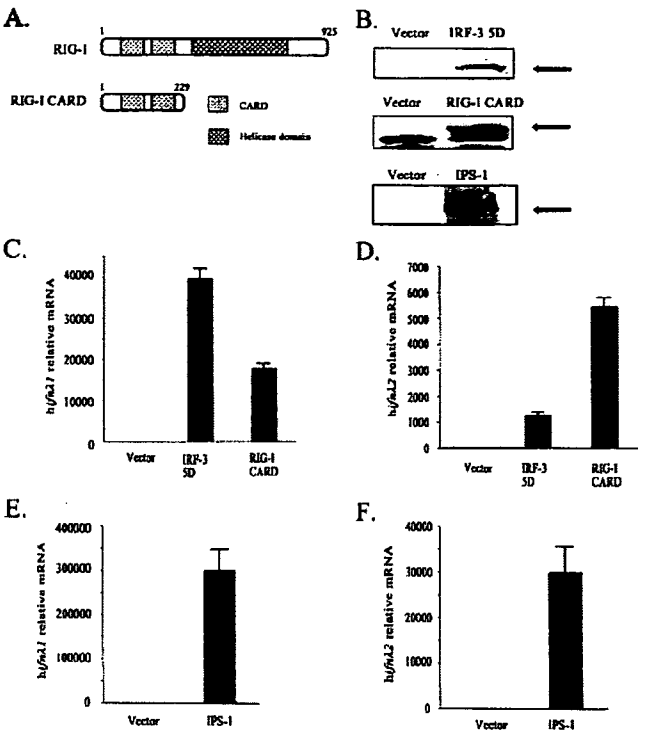

FIGURE 2. **Expression of a constitutively active IRF-3, RIG-I, and IPS-1 results in the activation of human *ifnλ1* and *ifnλ2*.** *A*, structure of full-length RIG-I and RIG-I CARD. *B*, transiently expressed IRF-3 5D, RIG-I CARD, and IPS-1 in 293T cells were monitored by SDS-PAGE followed by Western blotting. Shown is induction of endogenous human *ifnλ1* mRNA (*C* and *E*) and human *ifnλ2* mRNA (*D* and *F*) by ectopic expression of IRF-3 5D, RIG-I CARD, and IPS-1, respectively. The mRNA levels were determined as in Fig. 1.

FIGURE 3. **Identification of the transcription initiation site of the human *ifnλ1*.** *A*, HeLa cells were mock-treated or NDV-infected, and RACE PCR product was visualized by agarose electrophoresis. *B*, the RACE PCR fragment from *A* was cloned and sequenced to determine the transcription initiation site. The sequence of the RACE PCR product is aligned with the genomic sequence of the human *ifnλ1*. *Underbars* indicate the translation initiator ATG.

IFN-λ genes are regulated by IPS-1-mediated signaling, the major pathway triggered by viral replication.

Identification of the Transcription Initiation Site of the Human ifnλ1—The above results suggest the presence of one or more virus-inducible enhancer elements within the IFN-λ genes. To identify these elements, the transcription initiation site(s) of human *ifnλ1* was investigated by RACE. The RACE product was

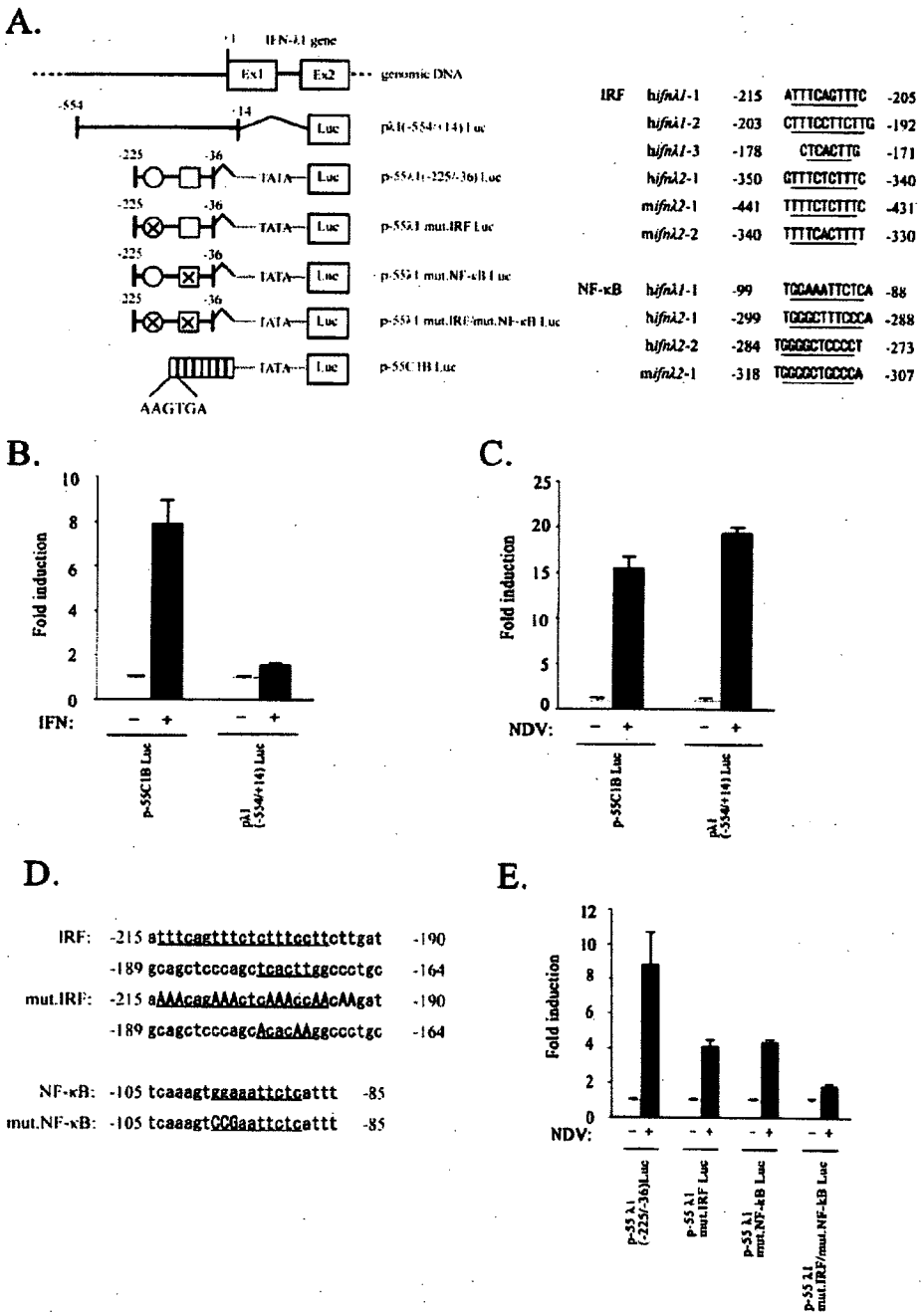

FIGURE 4. **Determination of *cis*-acting elements within the promoter of the human *ifnλ1*.** *A*, *left*, schematic representation of reporter constructs. This figure does not indicate the exact position of the elements. *Right*, binding sites for IRF and NF-κB (*underline*) in human *ifnλ1*, human *ifnλ2*, and mouse *ifnλ2* genes. The positions for the human *ifnλ1* are indicated as relative to the transcription initiation site (Fig. 3), whereas the positions of human *ifnλ2* and mouse *ifnλ2* are related to the translation initiation ATG. The reporters were transfected into L929 cells with pRL-TK as an internal control. The cells were mock-treated (−) or treated with 1000 units/ml of IFN-β for 12 h (+) (*B*) or infected with NDV for 12 h (+) (*C* and *E*) and were subjected to the Dual-Luciferase assay. *D*, nucleotide sequences of IRF and NF-κB binding sites present between −225 and −36 (*underline*); mutated nucleotides are indicated as *capital letters*. *Error bars* indicate the S.E. of triplicate transfections.

exclusively detected with NDV-infected RNA (Fig. 3*A*). The product was subcloned and sequenced. A random 10 clones had identical 5′ ends as shown in Fig. 3*B*. There was no TATA-like sequence at the expected position, thus we conclude that *ifnλ1* is a TATA-less gene.

Identification of the cis-Acting Regulatory Element of the Human ifnλ1—Next, we analyzed virus-inducible enhancer elements within the *ifnλ1*. We isolated the HeLa cell genomic fragment encompassing the human *ifnλ1* −554 to +14 relative to the transcription initiation site (see "Experimental Procedures") (Fig. 4*A*). The fragment was cloned into a firefly luciferase reporter gene (pλ1-(−554/+14)Luc) (Fig. 4*A*). For comparison, a reporter containing eight tandem repeats of the IRF-binding motif (p-55C1BLuc) (Fig. 4*A*, *bottom*) was used. Although p-55C1BLuc was significantly activated by IFN-β treatment, pλ1-(−554/+14)Luc was not significantly affected by IFN-β treatment, consistent with the observation that IFN-λ is barely inducible (1/1000 of viral induction) by type I IFN *per se* (Fig. 4*B*) (22). In contrast, NDV infection strongly induced the activation of both p-55C1BLuc and pλ1-(−554/+14)Luc, showing that the isolated genomic fragment contains a virus-inducible enhancer (Fig. 4*C*).

Critical Function of IRF and NF-κB-binding Sites within the ifnλ1 Enhancer—Within the above fragment, we noted putative binding sites for IRF (−214 to −172) and NF-κB (−98 to −89) (Fig. 4*A*). It is worth noting that multiple IRF-binding sites and a NF-κB motif exist similar to the *ifnβ* enhancer. Also, corresponding motifs were found in the human *ifnλ2* (Fig. 4*A*, *right*). To examine the function of these motifs, we chemically synthesized the region (−225 to −36) of human *ifnλ1* and cloned it into the upstream of the basal promoter of human *ifnβ* fused to a firefly luciferase reporter gene (p-55Luc (18)). Fig. 4*E* shows that the synthetic fragment functions as a virus-inducible *cis*-element, suggesting that the synthetic fragment encompasses the regulatory element. Disruption of the binding sites for either IRF or NF-κB reduced the level of virus-induced gene expression, and simultaneous disruption of these binding sites resulted in further impaired viral induction (Fig. 4, *D* and *E*). These results indicate that these binding sites function as components of a virus-inducible enhancer.

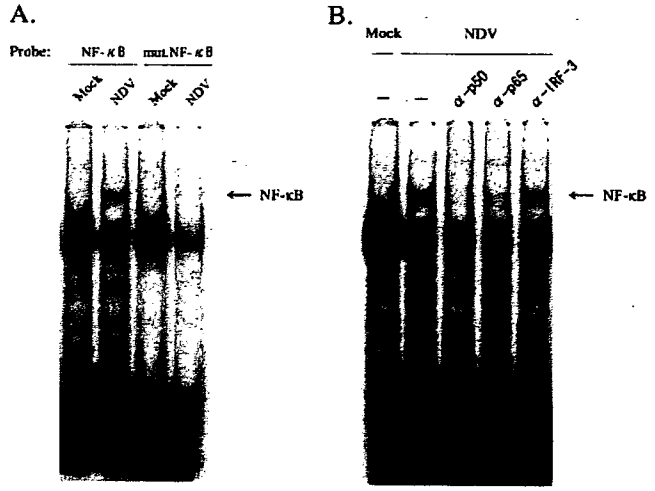

FIGURE 5. **p50/p65 NF-κB binds to the *ifnλ1* NF-κB motif.** *A*, HeLa cell extracts prepared from mock-treated or NDV-infected cells were subjected to EMSA using labeled *ifnλ1* NF-κB or mutated NF-κB oligonucleotide probes (see "Experimental Procedures"). *B*, NDV-infected extracts were each treated with the indicated antibody and were subjected to EMSA, as in *A*.

NF-κB Binds to the NF-κB Motif of ifnλ1—The above reporter assay suggested that the NF-κB motif is critical for IFN-λ gene induction. We tested NF-κB binding to the motif by EMSA (Fig. 5). NDV infection specifically induced binding activity to the wild-type but not to the mutated probe, suggesting that the motif is a functional NF-κB site (Fig. 5*A*). In addition, anti-p50 or -p65 antibody blocked the specific complex (Fig. 5*B*), suggesting that p50/p65 heterodimer binds to the *ifnλ1* NF-κB site.

DISCUSSION

The type I and III IFNs exhibit little structural conservation and are thought to have different origins. Indeed, types I and III IFNs elicit biological effects through interaction with distinct cell surface receptors. We found that, irrespective of their evolutional origin, IFN-λ genes are regulated by a mechanism common to type I IFNs. Our loss-of-function analyses revealed the involvement of IRF-3, TBK1, and RIG-I. Ectopic activation of IRF-3, RIG-I, and IPS-1 all activated type III IFN genes. These signaling molecules play a critical role in the virus-induced activation of type I IFN genes. Our search for a *cis*-element in the promoter of the human *ifnλ1* revealed a cluster of IRF-binding sites and a NF-κB-binding site as components of the virus-inducible enhancer. This is reminiscent of type I IFN enhancers, because multiple IRF sites critically regulate virus-inducible enhancers of IFN-α and -β, and a single κB site plays a critical role in the activation of IFN-β. Although IRF sites are potentially subject to regulation by IFN through IFN-stimulated gene factor 3, the expression of types I or III genes is little induced by IFN treatment *per se*. Thus, the common expression patterns of types I and III IFN genes are determined by the arrangements of these transcription factor-binding sites, which may be independently acquired through the evolution of the respective genes. Consistent with our finding, Osterlund *et al.* (23) report that IRF-3 binds to the IRF site predicted by a DNA affinity-binding assay. They also report the binding of NF-κB to the promoter region (at nucleotide position −264 to −256 from the transcription initiator site); however, removal of the predicted binding site did not affect the enhancer activity.[3] Instead, disruption of the other proximal NF-κB site (−98 to −89) significantly reduced the enhancer activity. Disruption of both IRF and NF-κB sites significantly reduced the transcriptional activity, but the mutant promoter exhibited weak activation, suggesting that unidentified *cis*-elements exist within the DNA fragment. In addition, they reported differential activation of *ifnλ1* and *ifnλ2*. Influenza A virus induces the expression of *ifnλ1* (but not *ifnλ2*), although Sendai virus induced production of high levels of both *ifnλ1* and *ifnλ2*. It is worth noting that, although putative binding sites for IRF and NF-κB are found in the promoter region of the *ifnλ2* (Fig. 4*A*, *right*), DNA sequence conservation to that of *ifnλ1* is low. Detailed analyses are necessary to elucidate the mechanism behind the virus-specific activation of type III IFN genes.

Because of the use of distinct receptors, types I and III IFNs likely do not signal identical biological outcomes in anti-viral and anti-cancer activities. Type I IFNs have been used to treat viral infections and certain cancers. The present study will help to establish a new strategy using IFN inducers. Developing inducers that commonly or differentially regulate types I and III IFN genes may enable us to manipulate the IFN system for therapeutic purposes.

REFERENCES

1. De Maeyer, E., and De Maeyer-Guignard, J. (1998) *Int. Rev. Immunol.* **17**, 53–73
2. Samuel, C. E. (2001) *Clin. Microbiol. Rev.* **14**, 778–809
3. Akira, S., and Takeda, K. (2004) *Nat. Rev. Immunol.* **4**, 499–511
4. Honda, K., Yanai, H., Takaoka, A., and Taniguchi, T. (2005) *Int. Immunol.* **17**, 1367–1378
5. Yoneyama, M., Kikuchi, M., Matsumoto, K., Imaizumi, T., Miyagishi, M., Taira, K., Foy, E., Loo, Y. M., Gale, M., Jr., Akira, S., Yonehara, S., Kato, A., and Fujita, T. (2005) *J. Immunol.* **175**, 2851–2858
6. Yoneyama, M., Kikuchi, M., Natsukawa, T., Shinobu, N., Imaizumi, T., Miyagishi, M., Taira, K., Akira, S., and Fujita, T. (2004) *Nat. Immunol.* **5**, 730–737
7. Kawai, T., Takahashi, K., Sato, S., Coban, C., Kumar, H., Kato, H., Ishii, K. J., Takeuchi, O., and Akira, S. (2005) *Nat. Immunol.* **6**, 981–988
8. Meylan, E., Curran, J., Hofmann, K., Moradpour, D., Binder, M., Bartenschlager, R., and Tschopp, J. (2005) *Nature* **437**, 1167–1172
9. Seth, R. B., Sun, L., Ea, C. K., and Chen, Z. J. (2005) *Cell* **122**, 669–682
10. Xu, L. G., Wang, Y. Y., Han, K. J., Li, L. Y., Zhai, Z., and Shu, H. B. (2005) *Mol. Cell* **19**, 727–740
11. Gitlin, L., Barchet, W., Gilfillan, S., Cella, M., Beutler, B., Flavell, R. A., Diamond, M. S., and Colonna, M. (2006) *Proc. Natl. Acad. Sci. U. S. A.* **103**, 8459–8464
12. Kato, H., Takeuchi, O., Sato, S., Yoneyama, M., Yamamoto, M., Matsui, K., Uematsu, S., Jung, A., Kawai, T., Ishii, K. J., Yamaguchi, O., Otsu, K., Tsujimura, T., Koh, C. S., Reis e Sousa, C., Matsuura, Y., Fujita, T., and Akira, S. (2006) *Nature* **441**, 101–105
13. Kotenko, S. V., Gallagher, G., Baurin, V. V., Lewis-Antes, A., Shen, M., Shah, N. K., Langer, J. A., Sheikh, F., Dickensheets, H., and Donnelly, R. P. (2003) *Nat. Immunol.* **4**, 69–77
14. Pestka, S., Krause, C. D., Sarkar, D., Walter, M. R., Shi, Y., and Fisher, P. B. (2004) *Annu. Rev. Immunol.* **22**, 929–979
15. Sheppard, P., Kindsvogel, W., Xu, W., Henderson, K., Schlutsmeyer, S., Whitmore, T. E., Kuestner, R., Garrigues, U., Birks, C., Roraback, J.,

[3] K. Onoguchi and T. Fujita, unpublished data.

Ostrander, C., Dong, D., Shin, J., Presnell, S., Fox, B., Haldeman, B., Cooper, E., Taft, D., Gilbert, T., Grant, F. J., Tackett, M., Krivan, W., McKnight, G., Clegg, C., Foster, D., and Klucher, K. M. (2003) *Nat. Immunol.* **4,** 63–68
16. Coccia, E. M., Severa, M., Giacomini, E., Monneron, D., Remoli, M. E., Julkunen, I., Cella, M., Lande, R., and Uze, G. (2004) *Eur. J. Immunol.* **34,** 796–805
17. Mori, M., Yoneyama, M., Ito, T., Takahashi, K., Inagaki, F., and Fujita, T. (2004) *J. Biol. Chem.* **279,** 9698–9702
18. Yoneyama, M., Suhara, W., Fukuhara, Y., Fukuda, M., Nishida, E., and Fujita, T. (1998) *EMBO J.* **17,** 1087–1095
19. Hemmi, H., Takeuchi, O., Sato, S., Yamamoto, M., Kaisho, T., Sanjo, H., Kawai, T., Hoshino, K., Takeda, K., and Akira, S. (2004) *J. Exp. Med.* **199,** 1641–1650
20. Sato, M., Suemori, H., Hata, N., Asagiri, M., Ogasawara, K., Nakao, K., Nakaya, T., Katsuki, M., Noguchi, S., Tanaka, N., and Taniguchi, T. (2000) *Immunity* **13,** 539–548
21. Kato, H., Sato, S., Yoneyama, M., Yamamoto, M., Uematsu, S., Matsui, K., Tsujimura, T., Takeda, K., Fujita, T., Takeuchi, O., and Akira, S. (2005) *Immunity* **23,** 19–28
22. Ank, N., West, H., Bartholdy, C., Eriksson, K., Thomsen, A. R., and Paludan, S. R. (2006) *J. Virol.* **80,** 4501–4509
23. Osterlund, P., Veckman, V., Siren, J., Klucher, K. M., Hiscott, J., Matikainen, S., and Julkunen, I. (2005) *J. Virol.* **79,** 9608–9617

THE JOURNAL OF IMMUNOLOGY

CUTTING EDGE

Cutting Edge: Influenza A Virus Activates TLR3-Dependent Inflammatory and RIG-I-Dependent Antiviral Responses in Human Lung Epithelial Cells[1]

Ronan Le Goffic,[*†] *Julien Pothlichet,*[*†] *Damien Vitour,*[‡] *Takashi Fujita,*[§] *Eliane Meurs,*[‡] *Michel Chignard,*[*†] *and Mustapha Si-Tahar*[2*†]

Influenza A virus (IAV) triggers a contagious acute respiratory disease that causes considerable mortality annually. Recently, we established a role for the pattern-recognition TLR3 in the response of lung epithelial cells to IAV-derived dsRNA. However, additional nucleic acid-recognition proteins have lately been implicated as key viral sensors, including the RNA helicases retinoic acid-inducible gene-I (RIG-I) and melanoma differentiation-associated gene (MDA)-5. In this study, we investigated the respective role of TLR3 vs RIG-I/MDA-5 signaling in human respiratory epithelial cells infected by IAV using BEAS-2B cells transfected with vectors encoding either a dominant-negative form of TLR3 or of mitochondrial antiviral signaling protein (MAVS; a signaling intermediate of RIG-I and MDA-5), or with plasmids overexpressing functional RIG-I or MDA-5. We demonstrate that the sensing of IAV by TLR3 primarily regulates a proinflammatory response, whereas RIG-I (but not MDA-5) mediates both a type I IFN-dependent antiviral signaling and a proinflammatory response. The Journal of Immunology,* 2007, 178: 3368–3372.

Influenza A virus (IAV)[3] belongs to the orthomyxoviruses family and is the etiological agent of a contagious acute respiratory disease that causes considerable mortality annually. IAV triggers pulmonary inflammation and exacerbates chronic lung diseases, due to an infiltration of inflammatory cells and an increased airway hyperresponsiveness. Bronchial epithelial cells are the primary target and the principal host for IAV, and thus play an important role in the pathogenesis of this viral infection (1, 2). However, whereas many of the molecular events in IAV replication have been described, the underlying mechanisms by which interaction between epithelial cells and viral components triggers the inflammation process have yet to be fully characterized.

Although recently challenged by some authors (3, 4), the viral replicative intermediate dsRNA is considered critical for the outcome of influenza infection (reviewed in Refs. 5, 6). Thus, RT-PCR experiments and binding of anti-helical dsRNA Abs to viroplasm from whole cell extracts suggest that true dsRNA accumulates within IAV-infected cells. Moreover, synthetic dsRNA and dsRNA isolated from IAV-infected lungs are each able to induce both the local and systemic cytotoxic effects typical of this viral infection (7, 8). Consistently, we recently used an in vitro approach to establish a role for the host dsRNA-recognition receptor TLR3 in the immune response of lung epithelial cells to IAV (9), and we demonstrated that, in vivo, IAV-TLR3 interaction critically contributes to viral pathology (10).

Nonetheless, additional cellular nucleic acid-recognition proteins have lately been implicated as key sensors of viral infection. These include two caspase recruiting domain (CARD) containing, DExD/H family RNA helicases, i.e., the retinoic acid-inducible gene-I (RIG-I) protein and the melanoma differentiation-associated gene (MDA)-5 protein (also known as helicard) (11, 12). Thus, there are at least two receptor systems in place to detect a viral presence and mount an immune response. These receptors localize to different compartments within a cell and recognize distinct ligands. Indeed, whereas it is established that MDA-5, like TLR3, acts as a dsRNA sensor (13, 14), RIG-I was recently shown to be activated by single-stranded viral genomic RNA bearing a 5′ triphosphate end (3, 15). Once triggered by their respective agonist, TLR3, RIG-I, and MDA-5 activate intracellular signaling pathways that may all culminate in the induction of antiviral cytokines such as type I IFNs as well as proinflammatory mediators (11, 12, 16).

*Institut Pasteur, Unité de Défense Innée et Inflammation, Paris, France; †Institut National de la Santé et de la Recherche Médicale Unité 874, Paris, France; ‡Institut Pasteur, Unité Postulante des Hépacivirus, Paris, France; and §Department of Tumor Cell Biology, The Tokyo Metropolitan Institute of Medical Science, Tokyo, Japan

Received for publication November 28, 2006. Accepted for publication January 16, 2007.

The costs of publication of this article were defrayed in part by the payment of page charges. This article must therefore be hereby marked *advertisement* in accordance with 18 U.S.C. Section 1734 solely to indicate this fact.

[1] This work was partially funded by the Institut Pasteur through a Programme Transversal de Recherche (Grant 186). Part of the work was also generously supported by the Société de Pneumologie de Langue Française. R.L.G. is a recipient of a Bourse Roux awarded by the Institut Pasteur. J.P. and D.V. were financially supported by the French association Vaincre la Mucoviscidose and by the Agence Nationale de la Recherche sur le Sida, respectively.

[2] Address correspondence and reprint requests to Dr. Mustapha Si-Tahar, Unité de Défense Innée et Inflammation, Institut National de la Santé et de la Recherche Médicale Unité 874, Institut Pasteur, 25 rue du Dr. Roux, 75015 Paris, France. E-mail address: sitahar@pasteur.fr

[3] Abbreviations used in this paper: IAV, influenza A virus; CARD, caspase recruiting domain; MAVS, mitochondrial antiviral signaling protein; MOI, multiplicity of infection; IRF, IFN regulatory factor; DC, dendritic cell.

These apparent similarities raise a pivotal question as to whether TLR3 and RNA helicases have redundant function and whether their activation leads to similar biological consequences or whether different cellular responses are induced depending on the class of viral nucleic acid receptor triggered. To delineate the respective role of TLR3 vs RIG-I/MDA-5 in the respiratory mucosa infected by IAV, we generated a set of experimental cell systems that allowed us to establish that the sensing of IAV by these receptors differs and has only a partial redundant outcome. Indeed, TLR3 activation critically regulates the induction of a proinflammatory response, whereas RIG-I (but not MDA-5) activation mediates both a type I IFN-dependent antiviral signaling and a proinflammatory response.

Materials and Methods

Cell and culture conditions

The human bronchial epithelial cell line BEAS-2B was cultured as described previously (9).

Virus preparation

Influenza A/Scotland/20/74 (H3N2) virus was prepared as indicated in Ref. 9.

Cytokine ELISA

Human IL-8, IL-6, RANTES, and IFN-β concentrations were determined using DuoSet ELISA kits obtained from R&D Systems.

RT-PCR

Total RNA was extracted using a RNeasy kit (Qiagen). Reverse transcriptase was performed using 1 μg of total RNA. PCR was performed using specific primers (Proligo) for human 2′5′ OAS (sense, 5′-ACA GCT GAA AGC CTT TTG GA-3′; antisense, 5′-AGA CCC CTT TGG CTT GAG TT-3′), Mx1 (sense, 5′-GTG CAT TGC AGA AGG TCA GA-3′; antisense, 5′-CGG CTA ACG GAT AAG CAG AG-3′), Mx2 (sense, 5′-AAG CAG TAT CGA GGC AAG GA-3′; antisense, 5′-TCG TGC TCT GAA CAG TTT GG-3′), RIG-I (sense, 5′-AGG AAA ACT GGC CCA AAA CT-3′; antisense, 5′-TTT CCC CTT TTG TCC TTG TG-3′), MDA-5 (sense, 5′-GTG CAT GGA GGA GGA ACT GT-3′; antisense, 5′-GTT ATT CTC CAT GCC CCA GA-3′), and mitochondrial antiviral signaling protein (MAVS; also called Cardif, Visa, or IPS-1 (11, 12, 16)) (sense, 5′-GCA GCA GAA ATG AGG AGA CC-3′; antisense, 5′-AAA GGT GCC CTC GGA CTT AT-3′). As an internal control, we used primers for human β-actin (sense, 5′-AAG GAG AAG CTG TGC TAC GTC GC-3′; antisense, 5′-AGA CAG CAC TGT GTT GGC GTA CA-3′). Amplifications were performed in a Peltier thermal cycler apparatus (MJ Research).

Transfection of pulmonary epithelial cells

Stably transfected pZero-hTLR3 or control BEAS-2B cells were generated using either 500 ng of a vector expressing TLR3, from which the Toll/IL-1R domain is deleted and thus encoding a nonfunctional TLR3 molecule (purchased from InvivoGen), or a pcDNA3 vector (Invitrogen Life Technologies), respectively. The procedure used the FuGENE 6 transfection reagent (Roche Molecular Diagnostics), according to the manufacturer's instructions. Concerning the reporter gene studies, BEAS-2B cells or pZero-hTLR3 BEAS-2B were transiently transfected with 150 ng of a NF-κB- (provided by Dr. A. Israel, Pasteur Institute, Paris, France), IFN-β-, or an ISG56-luciferase-reporter plasmid (provided by Dr. J. Hiscott, McGill University, Montreal, Canada) and 50 ng of pRSV-β-Gal to control DNA uptake. Cotransfection experiments with plasmids expressing a dominant-negative form of MAVS (a gift from Dr. Z. Chen, University of Texas Southwestern Medical Center, Dallas, TX) or vectors overexpressing a functional form of either MDA-5 (a gift from Dr. S. Goodbourn, University of London, U.K) or RIG-I were performed by including 200 ng of each plasmid to the previous transfection mixture. After 24 h, cells were left untreated or stimulated with IAV (5×10^4 PFU; multiplicity of infection (MOI) = 1) for 18 h at 37°C. Luciferase activity was measured in cell lysates as described previously (9).

Statistical analysis

The statistical significance of differences between groups was tested using the unpaired Student's t test with a threshold of $p < 0.05$.

Results and Discussion

TLR3 mediates NF-κB, but not IFN regulatory factor (IRF)-3-dependent gene expression in human bronchial epithelial cells infected by IAV

Effective antiviral immunity essentially relies on the production of type I IFNs such as IFN-α and IFN-β. The expression of type I IFNs is strictly regulated by the activation of latent transcription factors, including NF-κB and IRF-3 (17). Type I IFNs subsequently activate in an autocrine and paracrine manner the expression of IFN-stimulated genes (ISGs), which further collectively inhibit viral replication and assembly and elicit an antiviral state in the host (17). In contrast, beyond its role in the immune response, NF-κB has a central position in promoting inflammation by stimulating the expression of genes that contribute to the pathogenesis of inflammatory products, including a variety of cytokines (18). As a result, NF-κB represents an important and very attractive therapeutic target for drugs to treat many inflammatory pathologies, including lung diseases (19).

To better understand the specific contribution of the viral nucleic acid sensor TLR3 vs RIG-I/MDA-5 in the pathogenesis as well as the immune response associated to IAV infection, we generated human bronchial epithelial BEAS-2B cells that were stably transfected either with a control plasmid (control cells) or with a vector encoding a dominant-negative, nonfunctional, form of TLR3 (pZero-hTLR3 cells). These cells were infected by 5×10^4 PFU of IAV, a virus amount previously shown to potently activate pulmonary epithelial cells (9), and were further analyzed for the induction of antiviral and inflammatory responses.

Fig. 1 shows that NF-κB-driven luciferase activity was barely detectable in IAV-infected pZero-hTLR3 cells in comparison to a strong reporter signal in control BEAS-2B cells (80 ± 4 and 686 ± 91 relative light units, respectively). The activity of the IFN-β promoter was strongly stimulated in IAV-infected control cells and stimulated to a lower, yet significant ($p < 0.004$) extent in pZero-hTLR3 cells. By contrast, IAV infection resulted in a similarly high stimulation of the IRF-3-dependent, IFN-independent, ISG56 promoter in both pZero-hTLR3 cells and control BEAS-2B cells ($p > 0.05$). To support this latter finding, the expression of three known IFN-stimulated antiviral genes (2′5′ oligoadenylate synthetase (2′5′OAS) and myxovirus resistance protein (Mx)1 and 2) was analyzed by RT-PCR in the two cell types. The three genes were hardly detectable in noninfected BEAS-2B cells (Fig. 1*D*) and pZero-hTLR3 cells (data not shown) but were clearly up-regulated after IAV infection, to a comparable expression level. Thus, densitometric analysis of the PCR gels indicated the following gene:β-actin ratio: Mx1 = 0.35 ± 0.10 vs 0.39 ± 0.29, Mx2 = 0.55 ± 0.05 vs 0.48 ± 0.02, and 2′5′OAS = 1.32 ± 0.08 vs 1.08 ± 0.05, in control and pZero-hTLR3 cells, respectively. Altogether, these results show that inactivation of TLR3 in human bronchial epithelial cells strongly impairs the NF-κB-dependent signaling pathway while leaving the IRF-3-dependent signaling pathway rather unaffected. This result is particularly noteworthy in regard to the fact that in myeloid cells, TLR3 strongly regulates both NF-κB as well as IRF-3-dependent signal transduction (11, 20).

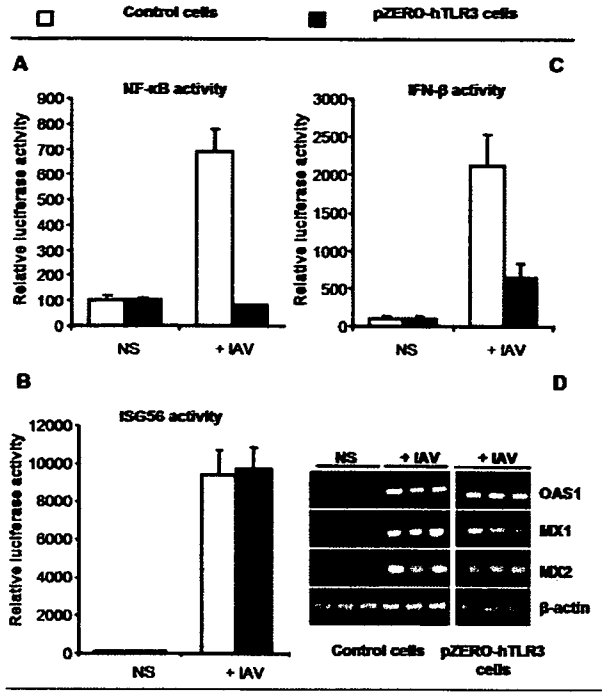

FIGURE 1. TLR3 mediates NF-κB, but not IRF-3-regulated gene expression in human bronchial epithelial cells. BEAS-2B cells stably expressing a vector encoding either a dominant-negative form of TLR3 (pZero-hTLR3) or an empty vector (control cells) were transfected with a NF-κB- (*A*), ISG56- (*B*), or IFN-β-luciferase reporter construct (*C*). Twenty-four hours after transfection, cells were infected or not by IAV (MOI = 1) during 18 h and cell lysates were prepared and assayed for luciferase activity. Results are mean ± SD of three distinct experiments. *D*, pZero-hTLR3 and control BEAS-2B cells were infected (+IAV) or not (NS) during 24 h. Total RNA was extracted, and OAS1, MX1, and MX2 mRNA expression was analyzed by RT-PCR. A representative result of three is shown.

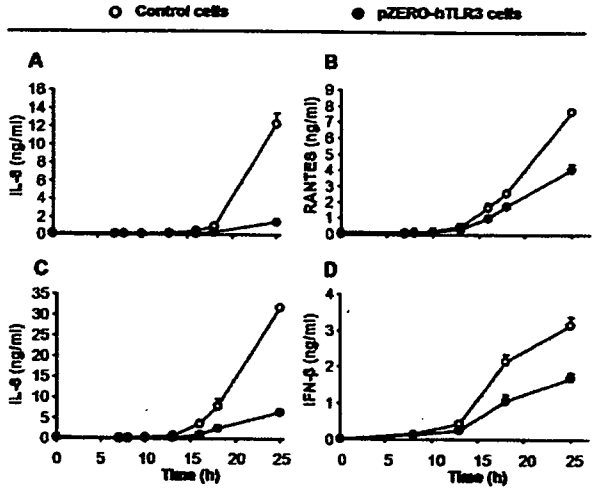

FIGURE 2. TLR3 plays a critical role in epithelial expression of proinflammatory cytokines. pZero-hTLR3 and control BEAS-2B cells were stimulated or not for various times by IAV (MOI = 1). Supernatant fluids were tested for IL-8 (*A*), RANTES (*B*), IL-6 (*C*), and IFN-β (*D*) by ELISA. Data are means ± SD of triplicate determinations of a representative experiment performed three times.

TLR3 plays a key role in the expression of proinflammatory cytokines in epithelial cells infected by IAV

The foregoing findings are important in regard to the numerous reports suggesting a major link between IAV-induced inflammatory cytokines and chemokines and injury of the lung tissue and disease severity (10, 21, 22). We measured, in the supernatants of pZero-hTLR3 and control cells, the secretion of an inflammatory cytokine whose maximal induction is essentially dependent on NF-κB, i.e., IL-8 (23) and an antiviral cytokine that is regulated mostly by IRF-3 (although additional transcriptional factors may play a role, including NF-κB), i.e., RANTES (24). Fig. 2, *A* and *B*, clearly shows that whereas IL-8 release is severely impaired in cells expressing the altered form of TLR3 (1.4 ± 0.1 and 12.3 ± 1.2 ng/ml in pZero-hTLR3 and control cells, respectively, at 24 h after IAV infection; $p < 0.001$), the secretion of RANTES is only partially inhibited (4.1 ± 0.4 and 7.6 ± 0.2 ng/ml in pZero-hTLR3 and control cells, respectively, at 24 h after IAV infection; $p < 0.005$). Similar results were obtained when considering the IAV-induced release of IL-6 and IFN-β, two cytokines that are regulated rather like IL-8 and RANTES, respectively (Fig. 2, *C* and *D*) (25, 26). The pivotal inflammatory role of TLR3 was confirmed by a still ongoing microarray study that is aimed to evaluate the overall impact of TLR3 on the transcriptome of IAV-infected pulmonary epithelial cells. Indeed, we found that among the genes that are specifically modulated by TLR3, many belong to a group of NF-κB-regulated genes, including GROα, GROβ, GROγ, and IL-8, but not IRF-3-driven genes such as IP-10, MIG, IFN-β, and I-TAC (data not illustrated).

RIG-I but not MDA-5 senses IAV and mediates both proinflammatory and antiviral signaling pathways

Although TLR3 has emerged as a key sensor of viral dsRNA, RIG-I and MDA-5 may also function as alternative pattern-recognition receptors of viral motifs (11, 12, 16). Guo et al. (27) recently indicated that RIG-I is important for induction of IFN by IAV. Siren et al. (28) reported that IAV does not activate HEK cells transfected by TLR3. This latter finding is markedly contradictory with our previous studies using both complementary in vitro and in vivo techniques that clearly demonstrated the major contribution of TLR3 in IAV sensing (9, 10). The same authors (28) reported that RIG-I and MDA-5 both mediate IAV-induced IFN synthesis. This finding also differs from other works that suggest a selective role for MDA-5 in the antiviral response to picornaviruses (29, 30).

In an attempt to clarify these discordant data, we aimed at dissecting the direct involvement of RIG-I and/or MDA-5 via MAVS in IAV detection. First, expression of those molecules was examined by RT-PCR in unstimulated or 5×10^4 PFU IAV-infected BEAS-2B cells for 24 h. Fig. 3*A* clearly shows that RIG-I, MDA-5, and MAVS are constitutively expressed in resting bronchial epithelial cells and that IAV challenge strikingly up-regulates the expression of RIG-I and MDA-5 but not that of MAVS. IAV up-regulates RNA helicases expression likely through an IFN feedback loop, as suggested by an experiment using BEAS-2B cells preincubated with either an isotype control Ab or a blocking anti-human type I IFN receptor before infection by IAV (MOI = 1; data not illustrated). The obtained data are consistent with previous works showing that RIG-I is overexpressed by inflammatory or viral stimuli including IFNs or IFN-inducing stimuli such as dsRNA, Sendai, or measles viruses and lipopolysaccharides (31–33). Next, we evaluated

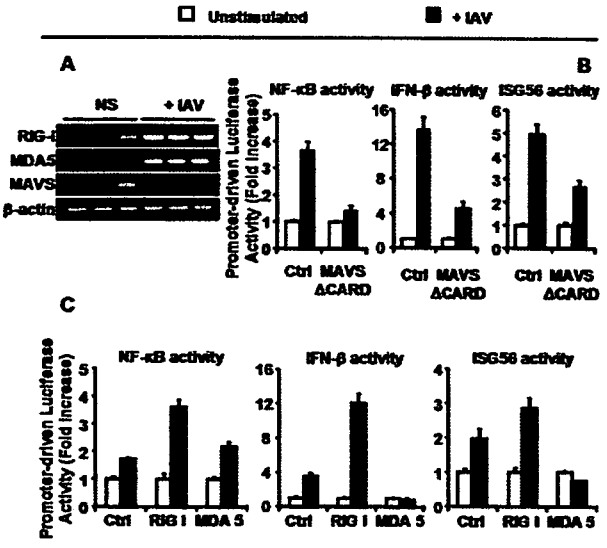

FIGURE 3. RIG-I, but not MDA-5, is involved in both NF-κB and IRF3-dependent signaling pathways induced by IAV. *A*, Representative RT-PCR showing RIG-I, MDA-5, and MAVS expression in resting (NS) and IAV-infected BEAS-2B cells (+IAV). *B*, BEAS-2B cells were cotransfected with either a NF-κB-, IFN-β-, or ISG56-luciferase reporter plasmid and a vector encoding a dominant-negative form of MAVS (MAVSΔCARD) or the respective control plasmid. *C*, BEAS-2B cells were cotransfected with the foregoing luciferase reporter plasmids as well as a vector overexpressing a functional form of either RIG-I or MDA-5 or the respective control plasmid. Twenty-four hours after transfection, cells were infected or not by IAV (MOI = 1) during 18 h and cell lysates were assayed for luciferase activity. Results are mean ± SD of three distinct experiments.

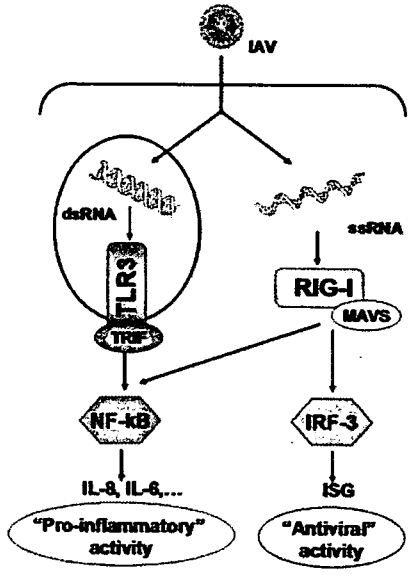

FIGURE 4. Dual recognition pathways of IAV-derived ribonucleic acids in pulmonary epithelial cells. This model suggests that the sensing of IAV by TLR3 and RNA helicases differs and has only a partial redundant outcome in bronchial epithelial cells. IAV infection leads to the exposure in the host cell of single-stranded (ss) genomic RNA and dsRNA (this latter being an intermediate of viral replication). Upon dsRNA binding within an endosomal compartment, TLR3 recruits the adaptor Toll/IL-1R domain-containing adaptor-inducing IFN-β (TRIF), which further activates NF-κB (10, 11). Upon recognition of ssRNA by RIG-I in the cytosol (3, 15), this complex interacts with MAVS to further activate both NF-κB and IRF-3. Hence, TLR3 activation may critically regulate the induction of a proinflammatory response, whereas RIG-I (but not MDA-5) activation may mediate both a type I IFN-dependent antiviral signaling and a proinflammatory response.

whether MAVS was involved in NF-κB and/or IRF-3 signaling pathways activated by IAV, using NF-κB, IFN-β, and ISG56 luciferase reporter plasmids as well as a vector encoding a dominant-negative form of MAVS (MAVSΔCARD) or a control plasmid. In comparison to BEAS-2B cells transfected with this latter vector, the foregoing signal transduction pathways were strongly reduced in cells transfected with MAVSΔCARD and infected by IAV (Fig. 3*B*). We next verified the upstream role of RIG-I or MDA-5 per se in the sensing and cell activation triggered by IAV using cells overexpressing a functional form of either receptor. Interestingly, we found that only RIG-I effectively activates NF-κB and IRF-3-dependent signaling pathways induced by IAV (Fig. 3*C*). It is of interest to notice in that regard that these results are in fair agreement with a previous study focusing on the mechanisms by which dendritic cells (DCs) are activated by viral stimuli. It showed key differences in the relative importance of signaling mediated by RIG-I vs TLRs in these leukocytes. Thus, the ability to induce antiviral response of conventional DCs was severely impaired in RIG-I$^{-/-}$ mice but not MyD88/TRIF$^{-/-}$ mice (which lack all TLR signaling). Remarkably, opposite results were observed in plasmacytoid DCs (34).

In conclusion, as shown in Fig. 4, we propose a dual pathway by which RIG-I (but not MDA-5) mediates both a type I IFN-dependent antiviral signaling and a proinflammatory response, whereas TLR3 especially regulates the induction of a proinflammatory response. Hence, these findings argue that RIG-I and TLR3 are only partially redundant and mediate specific host responses in human pulmonary epithelial cells. Accordingly, our results not only reinforce our previous findings dealing with IAV (9, 10), but also well support other investigations that demonstrated in models of phlebovirus or West Nile virus infection that TLR3 has a negative impact on viral disease by producing a number of selected proinflammatory chemokines and cytokines (35, 36). More important, the present study may help to elucidate the pathogenesis of IAV infection and thereby contribute to the design of molecules targeting TLR3 to prevent the excessive host inflammatory response produced by this virus.

Acknowledgments

We are grateful to Drs. Z. Chen (University of Texas Southwestern Medical Center, Dallas, TX) and S. Goodbourn (University of London, U.K.) for providing the MAVSΔCARD and MDA-5 plasmids, respectively. We also thank V. Lorin, Dr. N. Escriou, and Prof. S. van der Werf (Unité de Génétique Moléculaire des Virus Respiratoires, Institut Pasteur, Paris, France) for providing the IAV.

Disclosures

The authors have no financial conflict of interest.

References

1. Message, S. D., and S. L. Johnston. 2004. Host defense function of the airway epithelium in health and disease: clinical background. *J. Leukocyte Biol.* 75: 5–17.
2. Tamura, S., and T. Kurata. 2004. Defense mechanisms against influenza virus infection in the respiratory tract mucosa. *Jpn. J. Infect. Dis.* 57: 236–247.
3. Pichlmair, A., O. Schulz, C. P. Tan, T. I. Naslund, P. Liljestrom, F. Weber, and C. Reis e Sousa. 2006. RIG-I-mediated antiviral responses to single-stranded RNA bearing 5′-phosphates. *Science* 314: 997–1001.
4. Weber, F., V. Wagner, S. B. Rasmussen, R. Hartmann, and S. R. Paludan. 2006. Double-stranded RNA is produced by positive-strand RNA viruses and DNA viruses but not in detectable amounts by negative-strand RNA viruses. *J. Virol.* 80: 5059–5064.

5. Jacobs, B. L., and J. O. Langland. 1996. When two strands are better than one: the mediators and modulators of the cellular responses to double-stranded RNA. *Virology* 219: 339–349.
6. Majde, J. A. 2000. Viral double-stranded RNA, cytokines, and the flu. *J. Interferon Cytokine Res.* 20: 259–272.
7. Fang, J., S. Bredow, P. Taishi, J. A. Majde, and J. M. Krueger. 1999. Synthetic influenza viral double-stranded RNA induces an acute-phase response in rabbits. *J. Med. Virol.* 57: 198–203.
8. Kimura-Takeuchi, M., J. A. Majde, L. A. Toth, and J. M. Krueger. 1992. The role of double-stranded RNA in induction of the acute-phase response in an abortive influenza virus infection model. *J. Infect. Dis.* 166: 1266–1275.
9. Guillot, L., R. Le Goffic, S. Bloch, N. Escriou, S. Akira, M. Chignard, and M. Si-Tahar. 2005. Involvement of Toll-like receptor 3 in the immune response of lung epithelial cells to double-stranded RNA and influenza A virus. *J. Biol. Chem.* 280: 5571–5580.
10. Le Goffic, R., V. Balloy, M. Lagranderie, L. Alexopoulou, N. Escriou, R. Flavell, M. Chignard, and M. Si-Tahar. 2006. Detrimental contribution of the Toll-like receptor (TLR)3 to influenza A virus-induced acute pneumonia. *PLoS Pathog.* 2: e53.
11. Meylan, E., J. Tschopp, and M. Karin. 2006. Intracellular pattern recognition receptors in the host response. *Nature* 442: 39–44.
12. Seth, R. B., L. Sun, and Z. J. Chen. 2006. Antiviral innate immunity pathways. *Cell Res.* 16: 141–147.
13. Alexopoulou, L., A. C. Holt, R. Medzhitov, and R. A. Flavell. 2001. Recognition of double-stranded RNA and activation of NF-κB by Toll-like receptor 3. *Nature* 413: 732–738.
14. Kang, D. C., R. V. Gopalkrishnan, Q. Wu, E. Jankowsky, A. M. Pyle, and P. B. Fisher. 2002. *mda-5*: an interferon-inducible putative RNA helicase with double-stranded RNA-dependent ATPase activity and melanoma growth-suppressive properties. *Proc. Natl. Acad. Sci. USA* 99: 637–642.
15. Hornung, V., J. Ellegast, S. Kim, K. Brzozka, A. Jung, H. Kato, H. Poeck, S. Akira, K. K. Conzelmann, M. Schlee, et al. 2006. 5′-Triphosphate RNA is the ligand for RIG-I. *Science* 314: 994–997.
16. Akira, S. 2006. TLR signaling. *Curr. Top. Microbiol. Immunol.* 311: 1–16.
17. Honda, K., A. Takaoka, and T. Taniguchi. 2006. Type I interferon [correction of inteferon] gene induction by the interferon regulatory factor family of transcription factors. *Immunity* 25: 349–360.
18. Li, Q., and I. M. Verma. 2002. NF-κB regulation in the immune system. *Nat. Rev. Immunol.* 2: 725–734.
19. Park, G. Y., and J. W. Christman. 2006. Nuclear factor κB is a promising therapeutic target in inflammatory lung disease. *Curr. Drug Targets* 7: 661–668.
20. Sen, G. C., and S. N. Sarkar. 2005. Transcriptional signaling by double-stranded RNA: role of TLR3. *Cytokine Growth Factor Rev.* 16: 1–14.
21. Julkunen, I., T. Sareneva, J. Pirhonen, T. Ronni, K. Melen, and S. Matikainen. 2001. Molecular pathogenesis of influenza A virus infection and virus-induced regulation of cytokine gene expression. *Cytokine Growth Factor Rev.* 12: 171–180.
22. Van Reeth, K. 2000. Cytokines in the pathogenesis of influenza. *Vet. Microbiol.* 74: 109–116.
23. Smith, R. S., E. R. Fedyk, T. A. Springer, N. Mukaida, B. H. Iglewski, and R. P. Phipps. 2001. IL-8 production in human lung fibroblasts and epithelial cells activated by the *Pseudomonas* autoinducer *N*-3-oxododecanoyl homoserine lactone is transcriptionally regulated by NF-κB and activator protein-2. *J. Immunol.* 167: 366–374.
24. Lin, R., C. Heylbroeck, P. Genin, P. M. Pitha, and J. Hiscott. 1999. Essential role of interferon regulatory factor 3 in direct activation of RANTES chemokine transcription. *Mol. Cell. Biol.* 19: 959–966.
25. Goodbourn, S. 1990. The regulation of β-interferon gene expression. *Semin. Cancer Biol.* 1: 89–95.
26. Vanden Berghe, W., L. Vermeulen, G. De Wilde, K. De Bosscher, E. Boone, and G. Haegeman. 2000. Signal transduction by tumor necrosis factor and gene regulation of the inflammatory cytokine interleukin-6. *Biochem. Pharmacol.* 60: 1185–1195.
27. Guo, Z., L. M. Chen, H. Zeng, J. A. Gomez, J. Plowden, T. Fujita, J. M. Katz, R. O. Donis, and S. Sambhara. 2006. NS1 protein of influenza A virus inhibits the function of intracytoplasmic pathogen sensor, RIG-I. *Am. J. Respir. Cell Mol. Biol.* In press.
28. Siren, J., T. Imaizumi, D. Sarkar, T. Pietila, D. L. Noah, R. Lin, J. Hiscott, R. M. Krug, P. B. Fisher, I. Julkunen, and S. Matikainen. 2006. Retinoic acid inducible gene-I and *mda-5* are involved in influenza A virus-induced expression of antiviral cytokines. *Microbes Infect.* 8: 2013–2020.
29. Gitlin, L., W. Barchet, S. Gilfillan, M. Cella, B. Beutler, R. A. Flavell, M. S. Diamond, and M. Colonna. 2006. Essential role of mda-5 in type I IFN responses to polyriboinosinic:polyribocytidylic acid and encephalomyocarditis picornavirus. *Proc. Natl. Acad. Sci. USA* 103: 8459–8464.
30. Kato, H., O. Takeuchi, S. Sato, M. Yoneyama, M. Yamamoto, K. Matsui, S. Uematsu, A. Jung, T. Kawai, K. J. Ishii, et al. 2006. Differential roles of MDA5 and RIG-I helicases in the recognition of RNA viruses. *Nature* 441: 101–105.
31. Berghall, H., J. Siren, D. Sarkar, I. Julkunen, P. B. Fisher, R. Vainionpaa, and S. Matikainen. 2006. The interferon-inducible RNA helicase, mda-5, is involved in measles virus-induced expression of antiviral cytokines. *Microbes Infect.* 8: 2138–2144.
32. Komuro, A., and C. M. Horvath. 2006. RNA and virus-independent inhibition of antiviral signaling by RNA helicase LGP2. *J. Virol.* 80: 12332–12342.
33. Matikainen, S., J. Siren, J. Tissari, V. Veckman, J. Pirhonen, M. Severa, Q. Sun, R. Lin, S. Meri, G. Uze, et al. 2006. Tumor necrosis factor α enhances influenza A virus-induced expression of antiviral cytokines by activating RIG-I gene expression. *J. Virol.* 80: 3515–3522.
34. Kato, H., S. Sato, M. Yoneyama, M. Yamamoto, S. Uematsu, K. Matsui, T. Tsujimura, K. Takeda, T. Fujita, O. Takeuchi, and S. Akira. 2005. Cell type-specific involvement of RIG-I in antiviral response. *Immunity* 23: 19–28.
35. Gowen, B. B., J. D. Hoopes, M. H. Wong, K. H. Jung, K. C. Isakson, L. Alexopoulou, R. A. Flavell, and R. W. Sidwell. 2006. TLR3 deletion limits mortality and disease severity due to phlebovirus infection. *J. Immunol.* 177: 6301–6307.
36. Wang, T., T. Town, L. Alexopoulou, J. F. Anderson, E. Fikrig, and R. A. Flavell. 2004. Toll-like receptor 3 mediates West Nile virus entry into the brain causing lethal encephalitis. *Nat. Med.* 10: 1366–1373.

Rapid Communication

NS1 Protein of Influenza A Virus Inhibits the Function of Intracytoplasmic Pathogen Sensor, RIG-I

Zhu Guo, Li-mei Chen, Hui Zeng, Jorge A. Gomez, Julie Plowden, Takashi Fujita, Jacqueline M. Katz, Ruben O. Donis, and Suryaprakash Sambhara

Influenza Division, Centers for Disease Control and Prevention, Atlanta, Georgia; and Laboratory of Molecular Genetics, Institute for Virus Research, Kyoto University, Kyoto, Japan

Retinoic acid–inducible gene I (RIG-I) has recently been identified as one of the key intracellular sensors of virus infection. RIG-I binds to cytosolic double-stranded RNA and initiates a signaling cascade that leads to the activation of transcription factors required for expression of type I interferon (IFN-I). Previous evidence suggests that nonstructural protein 1 (NS1) encoded by influenza A virus (IAV) suppresses IFN-I secretion in virus-infected cells by an unknown mechanism. In the present study, we demonstrate that RIG-I is required for induction of IFN-I in an IAV-infected human lung epithelial cell line. Knockdown of RIG-I expression by RNA interference greatly impairs production of IFN-β in cells infected with different strains of wild-type IAV. Furthermore, co-expression of IAV NS1 down-regulates production of IFN-β induced by RIG-I agonists, and ectopic expression of RIG-I inhibits the replication of IAV. These results provide further information on the mechanism by which IAV NS1 antagonizes the host antiviral response.

CLINICAL RELEVANCE

Our findings indicate the potential clinical utility of RIG-I–based therapeutic strategies to prevent and treat infections caused by seasonal and pandemic influenza viruses.

The innate immune system is the host's first line of defense against a variety of pathogens. One of the major mechanisms for rapid initiation of host innate immune responses is to recognize conserved motifs or pathogen-associated molecule patterns (PAMPs) unique to microorganisms by pattern recognition receptors, such as Toll-like receptors (TLRs; 1). Upon recognition of PAMPs, TLRs activate signaling pathways that lead to secretion of proinflammatory cytokines, such as type I interferon (IFN-I), that are essential in antiviral immunity. Viral infection is generally associated with double-stranded RNA (dsRNA) production. IFN-I is induced by ligation of extracellular dsRNA, lipopolysaccharide, single-stranded RNA (ssRNA), and unmethylated CpG DNA to TLR3, TLR4, TLR7, and TLR9, respectively (1). TLR3 and TLR4 act through a Myd88-independent pathway, while TLR7 and TLR9 appear to use Myd88 as an adaptor protein for IFN signaling. In addition to TLR-dependent pathways, IFN-I is also induced by retinoic acid–inducible gene I (RIG-I) through recognition of intracellular dsRNA, a component or replication product of many RNA viruses (2). RIG-I contains two caspase recruitment domains (CARDs) at its N-terminus and a DExD/H box RNA helicase domain at its C-terminus. RIG-I interacts with dsRNA through its helicase domain and initiates IFN production in an ATPase-dependent manner (2). RIG-I CARD-mediated signaling results in the activation of IRF-3 and NF-κB.

Several human viruses, including hepatitis C virus (HCV, 3), vaccinia virus (4), Ebola virus (5), and influenza virus (6), have evolved strategies to target and inhibit distinct steps in the early signaling events that lead to IFN-I induction, indicating the importance of IFN-I in the host's antiviral response. The viral protease NS3/4A encoded by HCV has recently been shown to block the activation of IRF-3 by targeting multiple signaling steps. NS3/4A inactivates TRIF and IPS-1, adaptor proteins in TLR3- and RIG-I–dependent pathway, respectively, to prevent IFN-I production (3, 7, 8). The role of nonstructural protein 1 (NS1) of influenza A virus (IAV) as an IFN antagonist is evidenced by the hyper-induction of IFN-I in response to IAV lacking the NS1 gene (delNS1 virus) as compared with wild-type virus infection (6, 9, 10). In addition, expression of NS1 inhibits activation of IRF-3 (6). It is suggested that sequestering of viral dsRNA by NS1 during virus replication prevents access of host dsRNA sensors (6). However, the mechanisms by which NS1 antagonizes IFN-I response to IAV infection are still not fully understood. We now report that RIG-I is required for induction of IFN-I in response to IAV, and that NS1 suppresses production of IFN-I by targeting and inactivating the RIG-I–dependent signaling pathway.

MATERIALS AND METHODS

Cell Lines and Viruses

A549 and 293T cells were grown in Dulbecco's modified Eagle's medium (Life Technologies, Grand Island, NY) supplemented with 10% fetal bovine serum (HyClone Laboratories, Logan, UT), 100 U/ml penicillin, and 100 μg/ml streptomycin. Influenza viruses A/Puerto Rico/8/34 (PR8; H1N1) and A/Panama/2007/99 (H3N2) were grown in 10-d-old embryonated hen's eggs at 33.5°C for 48 h, while a highly pathogenic avian influenza (HPAI) virus A/Vietnam/1203/2004 (H5N1) was grown in eggs at 37°C for 24 h. All experiments with HPAI virus were performed in a biosafety level 3 laboratory with enhancement. Unless

(Received in original form August 3, 2006 and in final form October 17, 2006)

The findings and conclusions in this report are those of the authors and do not necessarily represent the views of the Centers for Disease Control and Prevention/ the Agency for Toxic Substances and Disease Registry or the funding agency.

The work presented here was supported by a grant from National Vaccine Program Office (NVPO).

Correspondence and requests for reprints should be addressed to Dr. Suryaprakash Sambhara, Centers for Disease Control and Prevention, 1600 Clifton Road, MS: G16, Atlanta, GA 30333. E-mail: ssambhara@cdc.gov

This article has an online supplement, which is accessible from this issue's table of contents at www.atsjournals.org

Am J Respir Cell Mol Biol Vol 36. pp 263–269, 2007
Originally Published in Press as DOI: 10.1165/rcmb.2006-0283RC on October 19, 2006
Internet address: www.atsjournals.org

specified, infection of cells by virus was performed at a multiplicity of infection (MOI) of 1 plaque-forming unit (pfu) per cell in a 6-well plate without trypsin supplementation. Influenza viruses were quantified by plaque assay on MDCK cells.

Plasmids and Small Interfering RNA

The pCAGGS-myc-NS1 was constructed by cloning a full-length cDNA of segment 8 from influenza PR8 virus into expression vector pCAGGS with a fusion sequence encoding c-myc-tag located at the 5′ end of cloned cDNA. The splice acceptor sequence was mutated by overlap PCR. Constructs that express domains of NS1, pCAGGS-myc-NS1aa1–80 and pCAGGS-myc-NS1aa81–230, were derived from pCAGGS-myc-NS1. The pEF-FLAG-RIG-I, pEF-FLAG-N-RIG-I, and pEF-FLAG-C-RIG-I plasmids have been described (2). The (-110-IFN-β)-CAT, $(PRDIII\text{-}I)_3$-CAT, pEF-Bos-TRIF, and pCDNA3-IKKε were kindly provided by T. Maniatis, Harvard University, Cambridge, MA. The pUNO-hIPS1 was purchased from Invivogen (San Diego, CA). Predesigned small interfering RNA (siRNA) targeting human RIG-I (siRIG-I), human MDA5 (siMDA5), and control siRNA targeting luciferase (siLuc) were purchased from Dharmacon (Chicago, IL).

Real-Time RT-PCR

Real-time RT-PCR was performed as described previously (11). Two sets of PCR assays were performed for each sample using primers specific for cDNA of the following genes: RIG-I, IFN-β, TNF-α, ISG15, MxA, and GAPDH. PCR product from above genes was cloned into PCR-Blunt II-TOPO vector (Invitrogen, Carlsbad, CA) and the cloned constructs were used to create standard curves in real-time PCR. The cycle threshold of each sample was converted to copy number of cDNA per μg of RNA and was normalized to GAPDH quantity of the corresponding sample. Unless specified, all assays were performed at least three times from independent RNA preparations.

Transient Transfection

Transient transfections of plasmid were performed using FuGENE 6 transfection reagent from Roche (Indianapolis, IN) according to the manufacturer's protocols. For transient transfection of dsRNA into 293T cells, 0.2 μg of poly (I:C) (Sigma-Aldrich, St. Louis, MO) was transfected with Lipofectamine 2,000 (Invitrogen). Transient transfections of siRNA into A549 cells were conducted using DharmaFECT 1 (Dharmacon) according to the manufacturer's protocols.

Western Blot

Western blot was performed as described previously (11). Antibodies against FLAG-tag and β-actin were purchased from Sigma-Aldrich, and c-myc-tag from Invitrogen. Antibody against human RIG-I was purchased from IBL (Gunma, Japan). Antibody against human MDA5 was described previously (13).

RESULTS

RIG-I Is Required for IFN-β Response to IAV Infection in Lung Epithelial Cells

RIG-I has been identified as a receptor for dsRNA and is required for induction of type I IFN in response to infection by several RNA viruses (2). To determine whether RIG-I is required for IFN-I response to IAV infection, we knocked down the endogenous expression of RIG-I in the human lung epithelial cell line A549 by RNA interference (RNAi) technique, and infected cells with influenza virus 24 h later. Transfection of siRNA targeting RIG-I, but not a control siRNA targeting the luciferase gene, greatly reduced the level of IFN-β mRNA induced 16 h after infection with IAV, suggesting an essential role for RIG-I in IFN-I response to IAV infection in this human lung epithelial cell line (Figure 1A). Similarly, the induction of type I IFN-inducible genes, ISG15 and MxA, were greatly reduced in cells transfected with siRNA targeting RIG-I (Figures 1B and 1C). It has been shown that the RIG-I signaling pathway bifurcates to activate IRF-3 and NF-κB (2). To determine whether RIG-I plays a role in IAV-induced expression of NF-κB–responsive genes, we analyzed the expression level of TNF-α (12), in RIG-I knocked-down cells (Figure 1D). The induction level of TNF-α was also greatly reduced in cells transfected with siRNA targeting RIG-I, indicating that the signaling pathway leading to NF-κB activation by IAV infection might require RIG-I function. The importance of RIG-I in the IFN-I response to IAV infection was also demonstrated by IFN-β promoter and IRF-3-responsive promoter reporter assays. Consistent with the results from real-time RT-PCR, IFN-β promoter (IFN-β–CAT) (Figure 1E) or IRF-3–responsive promoter (PRDIII-I–CAT) (Figure 1F) reporter expression was decreased in RIG-I knocked-down cells as compared with controls. The specificity of RNAi was evidenced by the greatly reduced expression of RIG-I mRNA and protein only in cells transfected with siRNA targeting RIG-I (Figures 1G and 1H). Taken together, these data indicate that RIG-I is essential for induction of IFN-I and TNF-α in response to IAV infection, and that the induction activity involves activation of IRF-3 and NF-κB.

Melanoma differentiation–associated gene 5 (MDA5), an RNA helicase related to RIG-I, has been shown to share a common signaling cascade with RIG-I (13). To determine whether MDA5 plays a role similar to RIG-I in IFN-I response to IAV infection, we knocked down the endogenous expression of MDA5 in A549 cells by RNAi, and infected cells with IAV 24 h later. Expression of MDA5 was induced by IAV infection, and this induction was greatly reduced only in cells transfected with siRNA targeting MDA5 (Figure 2A). However, in comparison to RIG-I, transfection of siRNA targeting MDA5 only slightly affected the expression level of IFN-β, ISG15, MxA, and TNF-α induced by IAV infection (Figure 2B), suggesting that MDA5 might be inessential for IFN-I response to IAV infection in this human lung epithelial cell line.

An alternative approach to demonstrate the critical role of RIG-I in the IFN-I response to IAV infection relied on transient overexpression of FLAG-tagged RIG-I (Figure 3A). Transient transfection of a full-length RIG-I expression vector into 293T cells was sufficient to induce CAT expression from the IFN-β–CAT reporter in a dose-dependent manner. IAV infection further enhanced the level of induction, which might occur through enhanced expression of endogenous RIG-I after IAV infection. Similarly, endogenous expression of IFN-β, ISG15, MxA, and TNF-α (Figure 4B) was induced by transient overexpression of RIG-I in A549 cells, and their expression was also further induced by IAV infection (data not shown). The N-terminal domain of RIG-I (N-RIG-I) has been found to be constitutively active in inducing IFN-β, while the C-terminal domain (C-RIG-I) functions as a dominant negative inhibitor (2). To determine whether expression of C-RIG-I can block IAV-initiated IFN-β induction, 293T cells were co-transfected with a FLAG-tagged C-RIG-I expression vector and the IFN-β–CAT reporter construct, and infected with IAV 24 h later. The induction level of IFN-β reporter was inhibited by C-RIG-I in a dose-dependent manner (Figure 3A), confirming that C-RIG-I is a dominant-negative inhibitor for IFN-β induction by IAV infection and that RIG-I does play an important role in IFN-I response to IAV infection. The ectopic expression of RIG-I and C-RIG-I was confirmed by Western blot analysis (Figure 3B).

This is the first report demonstrating that RIG-I is required for IFN-I response to wild-type IAV infection in human epithelial

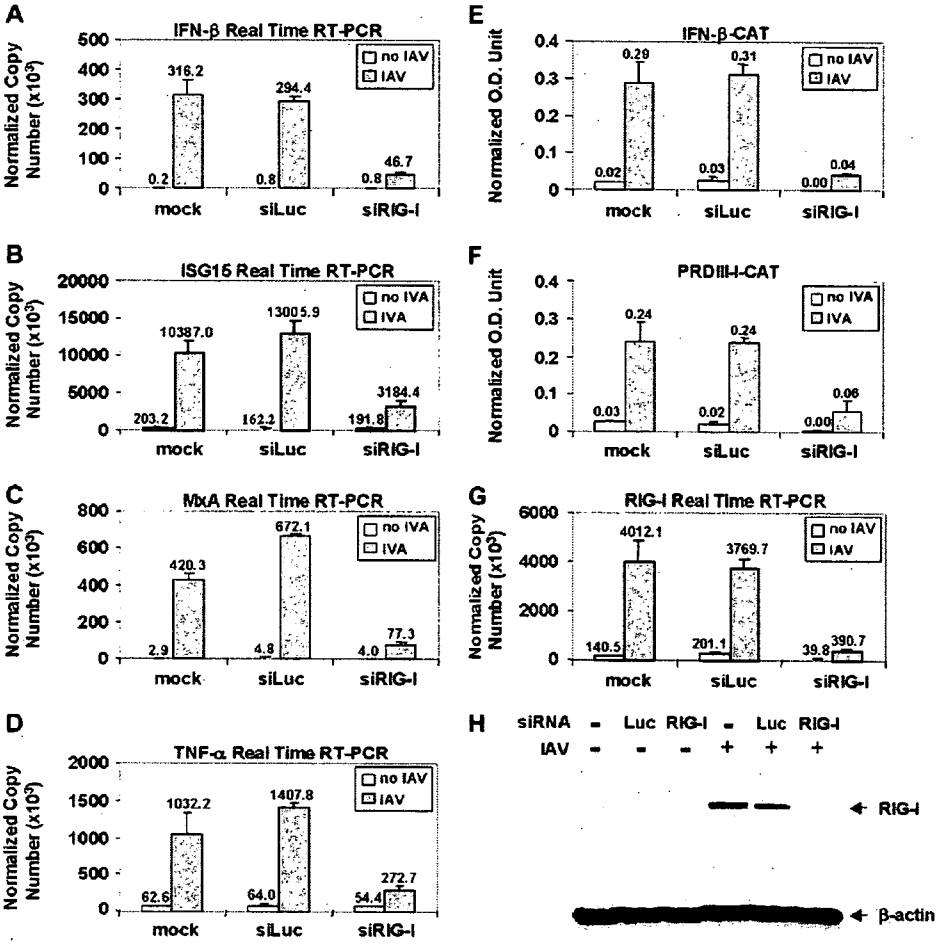

Figure 1. RIG-I is required for the induction of type I interferon against influenza A virus infection. A549 cells were transfected with siRNA targeting RIG-I (siRIG-I) or control siRNA targeting luciferase gene (siLuc). After 24 h incubation, transfected cells were infected with influenza virus A/Panama/2007/99 and incubated for 16 h. Total RNA was isolated, and real-time RT-PCR was performed to analyze IFN-β (*A*), ISG15 (*B*), MxA (*C*), TNF-α (*D*), and RIG-I (*G*) expression. For reporter assay and protein analysis, A549 cells were transiently co-transfected with siRNA and reporter plasmids as indicated, followed by infection with IAV PR8. Cell lysates were collected and analyzed by CAT ELISA (*E* and *F*), or by Western blot analysis using antibodies against RIG-I or β-actin (*H*). The average of three independent experiments is shown with SD.

cell lines. MDA5 is homologous to RIG-I and shares a common signaling cascade with RIG-I (13). Therefore, the function of MDA5 could compensate for the loss of RIG-I activity. However, our RNAi data demonstrate that knockdown of RIG-I expression greatly inhibits the IFN-I response to IAV infection (> 80% at mRNA level; Figure 1A). Furthermore, knockdown of MDA5 expression by RNAi only slightly represses the IFN-I response to IAV infection (Figure 2B). These results might indicate that MDA5 may not play a major role in the recognition of IAV, and the roles of RIG-I and MDA5 in innate response to virus infection may be differentiated in cells of lung epithelial cell lines (14).

RIG-I–Initiated Induction of Type I IFN Is Inhibited by NS1 Encoded by IAV

Influenza virus lacking the NS1 gene is a potent inducer of IFN-I and NS1 has been shown to inhibit activation of IRF-3 (6). However, the precise mechanism by which NS1 antagonizes induction of IFN-I remains unknown. The critical role of RIG-I in the IFN-β response to IAV infection prompted us to hypothesize that NS1 might target the RIG-I signaling pathway and inhibit production of IFN-I. To test this hypothesis, RIG-I expression construct and IFN-β–CAT reporter were co-transfected with various amounts of NS1 expression vector into A549 cells, and the activity of IFN-β promoter was analyzed by CAT ELISA. Transfection of the RIG-I expression vector alone greatly induced CAT expression from the IFN-β–CAT reporter, and co-transfection of the NS1 expression vector inhibited the induction activity of RIG-I in a dose-dependent manner (Figure 4A). Similarly, the endogenous expression of IFN-β, ISG15, MxA, and TNF-α was greatly induced by overexpression of RIG-I, and co-transfection of the NS1 expression vector almost completely blocked the induction (Figure 4B). It should be noted that transfection of NS1 expression vector alone caused a slight reduction (< 2-fold) in the basal level of IFN-β expression (*see* Figure E1 in the online supplement). However, the inhibitory function of NS1 on RIG-I signaling was not due to altered expression of RIG-I, as comparable levels of RIG-I expression were found in cells transfected with RIG-I or RIG-I plus NS1 expression constructs (Figure 4C).

Next, we determined whether NS1 could inhibit RIG-I activity in the presence of dsRNA. RIG-I expression vector and IFN-β promoter reporter plasmids were transfected with or without the NS1 expression vector into 293T cells. After 24 h of incubation, cells were transfected with dsRNA (poly [I:C]) and incubated for 8 h to induce IFN-I. The activity of IFN-β promoter was determined by CAT ELISA. Transfection of the RIG-I expression vector induced CAT expression driven by the IFN-β promoter, and the level of induction was further increased in cells transfected with poly (I:C), indicating that interaction of RIG-I with dsRNA enhanced the signaling activity of RIG-I (Figure 4D). Most importantly, the induction function of RIG-I was greatly inhibited by NS1 in the presence or absence of poly (I:C). CAT expression driven by IRF-3–responsive promoter

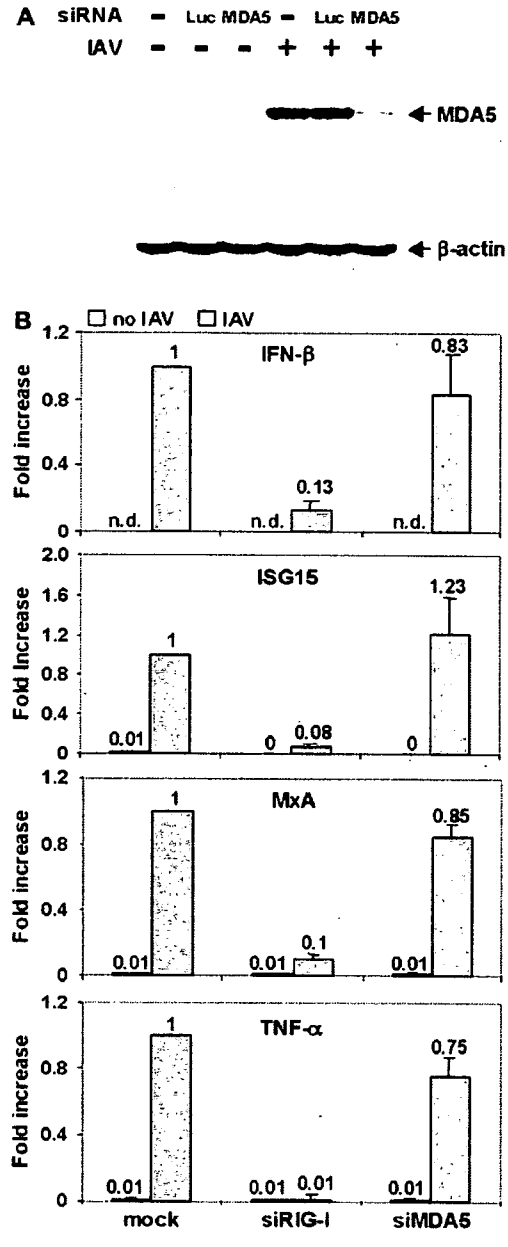

Figure 2. MDA5 is not essential for the induction of type I interferon against influenza A virus infection. A549 cells were transfected with siRNA targeting MDA5 (siMDA5), RIG-I (siRIG-I), or control siRNA targeting luciferase gene (siLuc). After 24 h incubation, transfected cells were infected with IAV PR8 and incubated for 16 h. Cell lysates were collected and analyzed by Western blot analysis using antibodies against MDA5 or β-actin (*A*). Total RNA was isolated, and real-time RT-PCR was performed to analyze the expression of IFN-β, ISG15, MxA, and TNF-α (*B*). The relative levels of mRNA expression were plotted as fold of increase with IAV-infected mock controls being set as 1-fold.

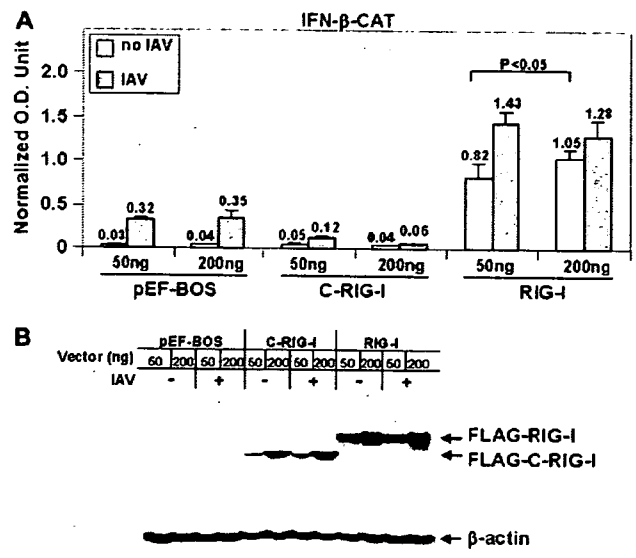

Figure 3. C-RIG-I functions as a dominant-negative inhibitor for IFN-β production induced by IAV infection. (*A*) 293T cells were transiently transfected with IFN-β promoter reporter plasmid DNA together with various amount of control vector pEF-BOS, or vectors that express FLAG-tagged C-terminal domain or full-length of human RIG-I. After 24 h incubation, cells were infected with IAV PR8 and incubated for another 24 h. Cell lysates were collected and a CAT ELISA was performed. The average of three independent experiments is shown with SD. (*B*) Samples tested by CAT ELISA from *A* were also analyzed by Western blot using antibodies against FLAG-tag or β-actin.

was also down-regulated by co-expression of NS1 (Figure 4E). Comparable levels of RIG-I expression were found in cells transfected with RIG-I or RIG-I plus NS1 expression constructs (Figure 4F). Also, transfection of NS1 expression vector had little effect on the expression level of β-galactosidase from pCDNA-LacZ, an RNA polymerase II–dependent reporter plasmid, suggesting that the inhibitory effect of NS1 on the expression of RNA polymerase II–dependent promoter reporter is minimal in our assay system (Figure E2). In addition, co-transfection of NS1 with IPS1, TRIF, or IKKε expression vectors failed to inhibit production of IFN-I that was induced by overexpression of these molecules, indicating the specificity of NS1 inhibitory activity on RIG-I pathway (Figure 4G).

To further determine the interaction between RIG-I and NS1, constructs that expressed domains of RIG-I or NS1 and IFN-β–CAT reporter plasmids were transfected with or without the full-length NS1 or RIG-I expression vectors into A549 cells (Figure 5A). Transfection of the N-RIG-I expression vector greatly induced CAT expression from the IFN-β promoter reporter, and co-transfection of the NS1 expression vector inhibited the induction activity of N-RIG-I. In addition, co-transfection of the constructs that expressed the N-terminus (amino acid 1–80), but not the C-terminus (amino acid 81–230) of NS1 with the RIG-I expression vector greatly repressed the induction of IFN-β–CAT reporter. Comparable levels of RIG-I expression were found in cells transfected with RIG-I or RIG-I plus NS1-domain expression vectors (Figure 5B).

NS1 of IAV is a multifunctional viral protein (15). Two cellular proteins that are required for the 3′-end processing of cellular pre-mRNAs, the 30-kD subunit of the cleavage and polyadenylation specificity factor (CPSF) and poly (A)-binding protein II (PABII), are bound and inactivated by IAV NS1, leading to decreased expression of the early type I IFN–independent antiviral genes (15). NS1 also inhibits the activation of another cellular antiviral gene, protein kinase R (PKR). Activation of PKR is known to phosphorylate the α-subunit of the translation initiation factor eIF2 to inhibit protein synthesis and therefore virus

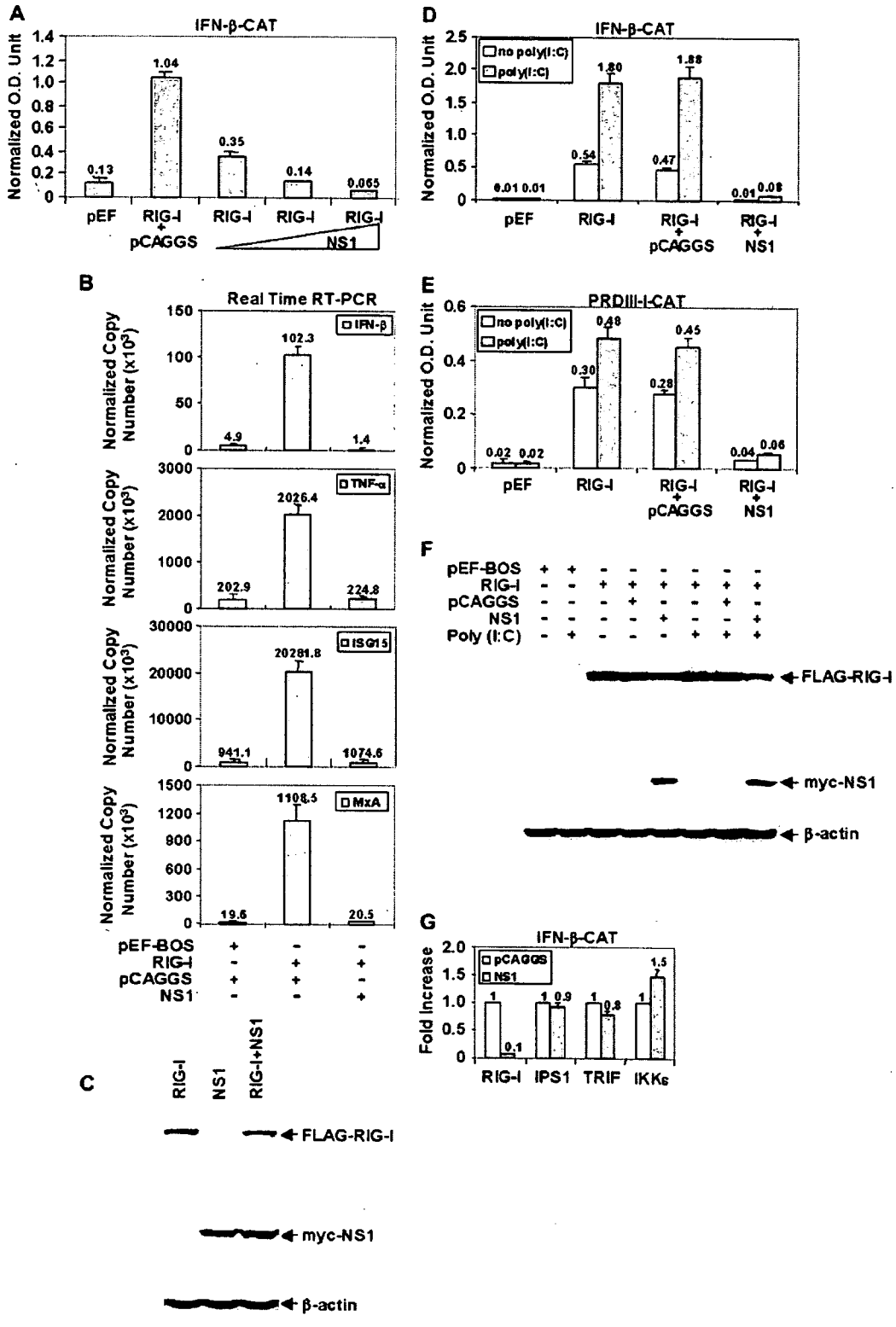

Figure 4. NS1 from influenza A virus antagonizes production of IFN-β induced by RIG-I. (*A*) IFN-β–CAT reporter and FLAG-tagged RIG-I expression vectors were transiently transfected with increased amounts of the myc-tagged NS1 expression vector into A549 cells. Cell lysates were collected 24 h after transfection and analyzed by CAT ELISA. (*B*) A549 cells were transfected with vectors that express FLAG-tagged RIG-I or myc-tagged NS1, or their corresponding control vectors pEF-BOS or pCAGGS as indicated. After 24 h of incubation, cells were collected and total RNA was isolated, followed by real-time RT-PCR analysis for the expression of IFN-β, ISG15, MxA, and TNF-α. (*C*) Western blot was performed to confirm the ectopic expression of RIG-I and NS1 using antibodies against FLAG-tag or myc-tag. (*D–F*) 293T cells were transiently transfected with indicated promoter reporter plasmids together with vectors that express FLAG-tagged RIG-I or myc-tagged NS1. After 24 h of incubation, cells were transfected with poly (I:C) and incubated for another 24 h. Cell lysates were collected and analyzed by CAT ELISA to determine activities of the IFN-β promoter (*D*) and IRF-3–responsive promoter (*E*), or analyzed by Western blot analysis using antibodies against FLAG-tag or myc-tag (*F*). (*G*) IFN-β–CAT reporter plasmids and vectors that expressed RIG-I, IPS1, TRIF, or IKKε were co-transfected with or without the myc-tagged NS1 expression vectors into A549 cells. Cell lysates were collected 24 h after transfection and analyzed by CAT ELISA. The relative levels of CAT expression were plotted as fold of increase with samples transfected with pCAGGS and adaptor expression vectors being set as 1-fold. The average of three independent experiments is shown with SD.

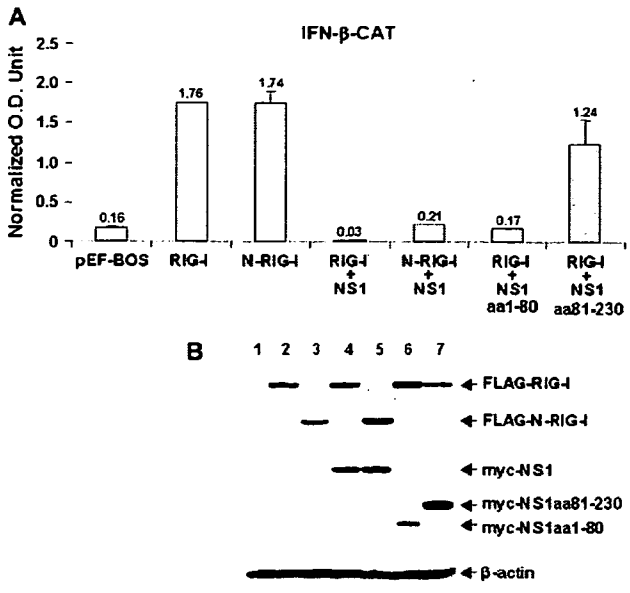

Figure 5. NS1 from IAV antagonizes RIG-I signaling through its N-terminal domain. A549 cells were transiently transfected with IFN-β–CAT reporter plasmids together with vectors that expressed FLAG-tagged RIG-I domains or myc-tagged NS1 domains. After 24 h of incubation, cell lysates were collected and analyzed by CAT ELISA (*A*), or analyzed by Western blot analysis using antibodies against FLAG-tag or myc-tag (*B*).

replication (15). Our data present further evidence that NS1 antagonizes the host antiviral response by targeting and inhibiting RIG-I signaling to block IRF-3 activation. It should be noted that NS1 inhibits the activity of RIG-I in the presence and absence of poly (I:C). The anti-IFN properties of IAV NS1

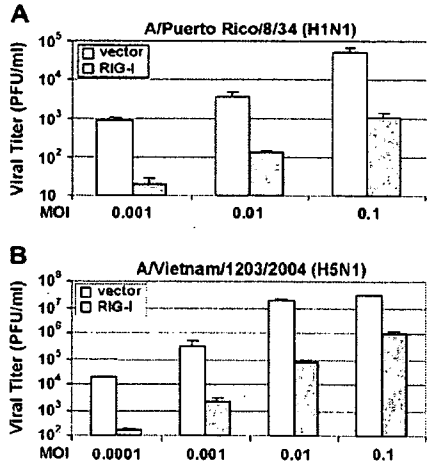

Figure 6. RIG-I inhibits replication of highly pathogenic avian influenza A virus. A549 cells were transiently transfected with control vector pEF-BOS or the vector that expresses full-length RIG-I. After 24 h of incubation, cells were infected with IAV PR8 (H1N1; *A*) or highly pathogenic avian IAV A/Vietnam/1203/2004 (H5N1; *B*) at various MOIs and incubated for another 24 h. Culture supernatants were collected and viral titers were determined by plaque assay on MDCK cells. The average of three independent experiments is shown with SD.

have been mapped to its N-terminal dsRNA-binding domain (10). Our data are consistent with the observation and indicate that the N-terminal domain of NS1 is sufficient to counteract RIG-I activity (Figure 5A).

RIG-I Inhibits IAV Replication

Increased expression of RIG-I has been shown to reduce the yield of vesicular stomatitis virus and encephalomyocarditis virus (2). To test whether RIG-I can inhibit replication of influenza virus, A549 cells were transiently transfected with the construct that expressed full-length RIG-I or its null expression control vector, and 24 h later were infected with IAV PR8 or highly pathogenic avian influenza virus A/Vietnam/1203/2004 (H5N1) at various MOI in the absence of trypsin. Compared with cells transfected with control vector, the yields for PR8 and H5N1 virus were reduced by 1 to 2 log of control in cells transfected with RIG-I expression vector (Figures 6A and 6B). Our results of inhibition of H1N1 and H5N1 IAV replication by RIG-I suggest the general capacity of RIG-I in anti-influenza function. Understanding the mechanism of how ectopic expression of human RIG-I induces type I IFN would provide insights for development of intervention strategy for viral infections.

Conflict of Interest Statement: None of the authors has a financial relationship with a commercial entity that has an interest in the subject of this manuscript.

Acknowledgments: The authors thank Dr. Tom Maniatis for sending reporter constructs (pEF-Bos-TRIF, pCDNA3-IKKε, [-110-IFN-β]-CAT, and [PRDIII-I]$_3$-CAT).

References

1. Kaisho T, Akira S. Toll-like receptor function and signaling. *J Allergy Clin Immunol* 2006;117:979–987.
2. Yoneyama M, Kikuchi M, Natsukawa T, Shinobu N, Imaizumi T, Miyagishi M, Taira K, Akira S, Fujita T. The RNA helicase RIG-I has an essential function in double-stranded RNA-induced innate antiviral responses. *Nat Immunol* 2004;5:730–737.
3. Li K, Foy E, Ferreon JC, Nakamura M, Ferreon AC, Ikeda M, Ray SC, Gale M Jr, Lemon SM. Immune evasion by hepatitis C virus NS3/4A protease-mediated cleavage of the Toll-like receptor 3 adaptor protein TRIF. *Proc Natl Acad Sci USA* 2005;102:2992–2997.
4. Smith EJ, Marie I, Prakash A, Garcia-Sastre A, Levy DE. IRF3 and IRF7 phosphorylation in virus-infected cells does not require double-stranded RNA-dependent protein kinase R or Ikappa B kinase but is blocked by Vaccinia virus E3L protein. *J Biol Chem* 2001;276:8951–8957.
5. Basler CF, Mikulasova A, Martinez-Sobrido L, Paragas J, Muhlberger E, Bray M, Klenk HD, Palese P, Garcia-Sastre A. The Ebola virus VP35 protein inhibits activation of interferon regulatory factor 3. *J Virol* 2003;77:7945–7956.
6. Talon J, Horvath CM, Polley R, Nakaya Y, Zheng H, Muster T, Garcia-Sastre A, Palese P. Activation of interferon regulatory factor 3 is inhibited by the influenza A virus NS1 protein. *J Virol* 2000;74:7989–7996.
7. Foy E, Li K, Sumpter R Jr, Loo YM, Johnson CL, Wang C, Fish PM, Yoneyama M, Fujita T, Lemon SM. Control of antiviral defenses through hepatitis C virus disruption of retinoic acid-inducible gene-I signaling. *Proc Natl Acad Sci USA* 2005;102:2986–2991.
8. Meylan E, Curran J, Hofmann K, Moradpour D, Binder M, Bartenschlager R, Tschopp J. Cardif is an adaptor protein in the RIG-I antiviral pathway and is targeted by hepatitis C virus. *Nature* 2005;437:1167–1172.
9. Donelan NR, Basler CF, Garcia-Sastre A. A recombinant influenza A virus expressing an RNA-binding-defective NS1 protein induces high levels of beta interferon and is attenuated in mice. *J Virol* 2003;77:13257–13266.
10. Wang X, Li M, Zheng H, Muster T, Palese P, Beg AA, Garcia-Sastre A. Influenza A virus NS1 protein prevents activation of NF-kappaB and induction of alpha/beta interferon. *J Virol* 2000;74:11566–11573.
11. Guo Z, Garg S, Hill KM, Jayashankar L, Mooney MR, Hoelscher M, Katz JM, Boss JM, Sambhara S. A distal regulatory region is required for constitutive and IFN-beta-induced expression of murine TLR9 gene. *J Immunol* 2005;175:7407–7418.

12. Collart MA, Baeuerle P, Vassalli P. Regulation of tumor necrosis factor alpha transcription in macrophages: involvement of four kappa B-like motifs and of constitutive and inducible forms of NF-kappa B. *Mol Cell Biol* 1990;10:1498–1506.
13. Yoneyama M, Kikuchi M, Matsumoto K, Imaizumi T, Miyagishi M, Taira K, Foy E, Loo YM, Gale M Jr, Akira S, *et al.* Shared and unique functions of the DExD/H-box helicases RIG-I, MDA5, and LGP2 in antiviral innate immunity. *J Immunol* 2005;175:2851–2858.
14. Kato H, Takeuchi O, Sato S, Yoneyama M, Yamamoto M, Matsui K, Uematsu S, Jung A, Kawai T, Ishii KJ, *et al.* Differential roles of MDA5 and RIG-I helicases in the recognition of RNA viruses. *Nature* 2006;441:101–105.
15. Krug RM, Yuan W, Noah DL, Latham AG. Intracellular warfare between human influenza viruses and human cells: the roles of the viral NS1 protein. *Virology* 2003;309:181–189.

***Note added in proof*:** After the submission of this manuscript, three additional groups reported NS1-mediated inhibition of RIG-I function.

Pichlmair A, Schulz O, Tan CP, Naslund TI, Liljestrom P, Weber F, Reis e Sousa C. RIG-I-mediated antiviral responses to single-stranded RNA bearing 5′-phosphates. *Science* Epub 2006 Oct 12.

Mibayashi M, Martinez-Sobrido L, Loo YM, Cardenas WB, Gale M Jr, Garcia-Sastre A. Inhibition of retinoic acid-inducible gene I-mediated induction of beta interferon by the NS1 protein of influenza A virus. *J Virology* Epub 2006 Nov 1.

Opitz B, Rejaibi A, Dauber B, Eckhard J, Vinzing M, Schmeck B, Hippenstiel S, Suttorp N, Wolff T. IFNbeta induction by influenza A virus is mediated by RIG-I which is regulated by the viral NS1 protein. *Cell Microbiol* Epub 2006 Nov 28.

Negative regulation of the RIG-I signaling by the ubiquitin ligase RNF125

Kei-ichiro Arimoto*, Hitoshi Takahashi*, Takayuki Hishiki*, Hideyuki Konishi*, Takashi Fujita†, and Kunitada Shimotohno*‡

*Department of Viral Oncology and †Department of Genetic and Molecular Biology, Institute for Virus Research, Kyoto University, Sakyo-ku, Kyoto 606-8507, Japan

Edited by Tak Wah Mak, University of Toronto, Toronto, ON, Canada, and approved March 16, 2007 (received for review December 25, 2006)

Retinoic acid-inducible gene I (*RIG-I*) plays a pivotal role in the regulation of cytokine production induced by pathogens. The RIG-I also augments the production of IFN and other cytokines via an amplification circuit. Because the production of cytokines is closely controlled, up- and down-regulation of RIG-I signaling also needs strict regulation. The mechanism of this regulation, however, remains elusive. Here, we found that RIG-I undergoes proteasomal degradation after conjugation to ubiquitin by RNF125. Further, RNF125 conjugates ubiquitin to MDA5, a family protein of RIG-I as well as IPS-1, which is also a downstream protein of RIG-I signaling that results in suppressing the functions of these proteins. Because RNF125 is enhanced by IFN, these functions constitute a negative regulatory loop circuit for IFN production.

innate immunity | signal transduction

Upon viral infection, host cells activate the innate immune signaling cascades critical for effective antiviral immune responses (1, 2). The viral components, such as viral DNA or RNA, are recognized by Toll-like receptors (TLRs) that stimulate the production of antiviral factors including cytokines and induce inflammatory and adaptive immune responses (1–8). In addition to TLR-dependent activation of innate immunity, retinoic acid-inducible gene I (*RIG-I*) and other proteins in this family can also detect viral components or dsRNA, inducing the production of cytokines necessary to activate innate and adaptive immune responses (9, 10). The RIG-I is a DExD/H box RNA helicase with two caspase-recruiting domain (CARD)-like sequences and a helicase domain that is required for its interaction with dsRNA. The CARD-like domains are responsible for activating downstream signaling (9) through interactions with IPS-1/MAVS/VISA/Cardif (11–13).

The rapid induction of type-1 IFN expression is the key event in the initiation of the innate antiviral response, and it requires the pathogen-inducible activation of transcription factors that function synergistically to induce gene expression (9, 14–16). Among members of the IFN regulatory factor family, IRF3 and IRF7 play essential roles in virus-induced type-1 IFN gene activation after infection (9, 13, 17, 18).

Activation of TLRs results in a proinflammatory response necessary to prevent the spread of infection. Limiting TLR signaling, however, is essential to prevent this protective response from causing injury to the host. Several regulatory mechanisms that suppress TLR signaling have been described in earlier reports (19–22). Regulation of the TLR-independent, RIG-I-mediated signaling pathway regulating IRF3; however, it is not well understood. Recently, A20, an NF-κB-inducible ubiquitin-editing protein able to inhibit TLR3- and Sendai virus-induced activation of the ISRE promoter (23) was shown to inhibit this signaling pathway (24).

To clarify the mechanisms underlying the negative regulation of RIG-I signaling, we searched for a Ubl E3 ligase that modifies RIG-I. The result of the search was the identification of RNF125 (*Homo sapiens* ring-finger protein 125, GenBank accession no. NM_017831), also named TRAC-1 (T cell RING protein identified in activation screen), an E3 ubiquitin ligase serving a positive regulatory role in T cell activation (25), that functioned as an E3 ligase for RIG-I ubiquitin conjugation. Ubiquitin-conjugated RIG-I was degraded in a proteasome-dependent manner. We also observed that RNF125 possessed the ability to conjugate ubiquitin to MDA5, a member of the RIG-I protein family, as well as IPS1/MAVS/VISA/Cardif (referred to as IPS1 hereafter), a protein downstream of RIG-I signaling, which also suppresses RIG-I mediated signaling.

Results

Isolation of RNF125 as an Interacting Protein with UbcH8. RIG-I is reported to be conjugated (ISGylated) to ISG15 (26). UBE1L and UbcH8 function as E1 and E2 enzymes for ISGylation, respectively. Cotransfection of 293FT cells with plasmids encoding UBE1L, UbcH8, and ISG15 promoted the ISGylation of RIG-I (data not shown). The UbcH8 functions as an E2 enzyme for both ubiquitin and ISG15 conjugation (16, 27–33). We made an attempt to isolate a candidate E3-ligase capable of conjugating ISG15 or ubiquitin to RIG-I. We hypothesized that this candidate E3-ligase would interact with UbcH8 because, under certain circumstances, the interaction of E2 enzymes and E3 ligases can be observed *in vitro* during the conjugation of ubiquitin-like protein (Ubl) (32, 34). Using a yeast-two hybrid screening, we isolated RNF125 as an interacting protein with UbcH8. RNF125, a RING motif containing proteins, can act as a ubiquitin E3 ligase (25). A schematic diagram of RNF125 and its mutants used in this paper are shown in Fig. 1*a*. We found that RIG-I interacted with RNF125 as well as UbcH8 (Fig. 1 *c* and *d*). We analyzed the regions of RIG-I interacting with RNF125 by using deletion mutants of RIG-I as well as the region of RNF125 interacting with RIG-I (Fig. 1 *e* and *f*). From this analysis, the CARD domain of RIG-I as well as the C-terminal region of RIG-I were found to interact with the N-terminal region of RNF125.

RNF125 Is an E3-Ligase for Conjugation of Ubiquitin to RIG-I. We analyzed whether the E3-ligase activity of RNF125 is responsible for the ubiquitination of RIG-I. When FLAG-RIG-I, HA-RNF125, and Myc-Ub were expressed in 293FT cells, ubiquitin conjugation to RIG-I was observed (Fig. 2*a*). The level of ubiquitination was low in the absence of ectopic RNF125 expression. The fact that RNF125 is the ubiquitin E3-ligase for

Author contributions: K.-i.A. and K.S. designed research; K.-i.A. and H.K. performed research; H.T., T.H., and T.F. contributed new reagents/analytic tools; K.-i.A., H.T., T.H., H.K., and K.S. analyzed data; and K.-i.A. and K.S. wrote the paper.

The authors declare no conflict of interest.

This article is a PNAS Direct Submission.

Abbreviations: CARD, caspase-recruiting domain; CHX, cycloheximide; MEF, mouse embryonic fibroblast; TLR, Toll-like receptor.

‡To whom correspondence should be addressed. E-mail: kshimoto@virus.kyoto-u.ac.jp.

This article contains supporting information online at www.pnas.org/cgi/content/full/0611551104/DC1.

www.pnas.org/cgi/doi/10.1073/pnas.0611551104

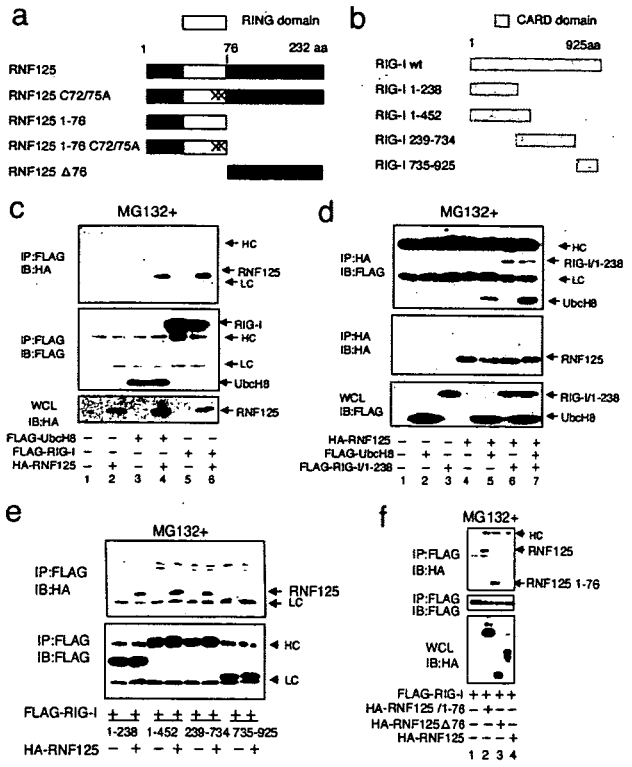

Fig. 1. Association of RNF125 with UbcH8 and RIG-I. (*a* and *b*) Schematic structure of RNF125, RIG-I, and their derivatives used in this work. "X" indicates site of cysteine residue substitution with alanine at the 72nd and 75th residues in RNF125. (*c* and *d*) Coimmunoprecipitation experiments. The 293FT cells were transfected as indicated. Thirty-six hours after transfection, protein associations were analyzed either by coimmunoprecipitation using anti-FLAG antibody, followed by Western blot using anti-HA antibody (*c*), or by coimmunoprecipitation using anti-HA antibody, followed by anti-FLAG antibody (*d*). (*e*) Analysis of the RIG-I domain that interacts with RNF125. Plasmids expressing various deletion mutants, including amino acids 1–238, 1–452, 239–734, and 735–925 of RIG-I fused to a FLAG epitope tag (*b*), were transfected into 293FT cells with or without a plasmid encoding HA-RNF125. Complex formation was examined by immunoprecipitation with an anti-FLAG antibody followed by immunoblotting using the anti-HA antibody (*Upper*). The amount of each RIG-I mutant in the complex is indicated (*Lower*). (*f*) Analysis of the association of RIG-I with RNF125 mutants. Plasmids as indicated were transfected into 293FT cells. The lysates were immunoprecipitated by using an anti-FLAG antibody, followed by blotting with the anti-HA antibody (*Top*). The quantity of FLAG-RIG-I in the immunocomplexes as well as the RNF125 and mutants in whole-cell lysates are also shown in *Middle* and *Bottom*, respectively. HC and LC indicate the heavy and light chains of human immunoglobulins, which are also indicated in the following figures. All cells in *c*–*f* were treated with MG132.

RIG-I was further confirmed by the suppression of endogenous RNF125 using siRNA. Transfection of cells with siRNF125–3 strongly suppressed the production of RNF125 mRNA, leading to a substantial reduction in RNF125 protein levels in 293FT cells (Fig. 2*b Upper*). In cells treated with siRNF125–3, with the exception of those treated with control siRNA, the levels of RIG-I polyubiquitination were substantially reduced (Fig. 2*b Lower*).

Analysis of the E3-Ligase Domain of RNF125 and a Target Region in RIG-I for Ubiquitination. To verify the role of the RNF125 RING domain in ubiquitin conjugation to RIG-I, we performed a mutational analysis. Although RIG-I could be conjugated to ubiquitin by WT RNF125 (Fig. 2*a*, lane 3), an RNF125 mutant [in which the 72nd and 75th cysteine residues were substituted with alanine (C72/75A)] was unable to mediate RIG-I ubiquitination (Fig. 2*a*, lane 4). A peptide encompassing the first 76 residues of RNF125 (1–76 aa), a region containing the intact RING domain, mediated ubiquitin conjugation similar to the WT RNF125. The mutant Cys-72 and Cys-75 in this peptide (1–76 aa C72/75A), however, completely abrogated its ubiquitin-conjugating activity (Fig. 2*a*, lane 6).

To verify the region of RIG-I conjugated to ubiquitin, we analyzed ubiquitin conjugation to FLAG-RIG-I mutants in cells coproducing HA-RNF125 and Myc-Ub (Fig. 2*c*). Peptides containing CARD domain of RIG-I, amino acids 1–238 (RIG-1/1–238) or 1–452 (RIG-I/1–452), were ubiquitinated at higher levels than intact RIG-I. In contrast, C-terminal RIG-I peptides, RIG-I/239–734 and RIG-I/735–925, were only weakly conjugated. Using the N-terminal region of RIG-I (RIG-I/1–238) as a substrate, we confirmed that RNF125, and not Efp (estrogen-responsive finger proteins), another ubiquitin E3 ligase, efficiently conjugated ubiquitin (data not shown), further supporting the conclusion that RNF125 acts as an E3 ligase for RIG-I.

Degradation of RIG-I Is Enhanced by the Expression of RNF125. Polyubiquitin was primarily conjugated to the N-terminal CARD-containing region of RIG-I (Fig. 2*c*). Steady-state levels of the ubiquitin-conjugated peptide containing the N-terminal region, RIG-I/1–238, were increased in cells treated with MG132, a proteasome inhibitor (Fig. 2*d*). These results suggest that RNF125-dependent RIG-I ubiquitination precedes proteasome-dependent degradation. Full-length RIG-I was also degraded with ectopic expression of RNF125 but not with the mutant C72/75A in 293FT cells (Fig. 2*e*). The levels of RIG-I were reduced as increasing amounts of RNF125 were expressed (Fig. 2*f*). Under these conditions, mRNA levels of RIG-I, GAPDH, p53, and tubulin remained unchanged. When cells were treated with MG132, the degradation of RIG-I was suppressed. These results clearly demonstrate that RNF125 acts as a ubiquitin E3-ligase regulating the cellular levels of RIG-I through proteasomal degradation. Proteasomal degradation of RIG-I was also observed in other cell types such as HeLa and HepG2 (data not shown).

Degradation of RIG-I is enhanced by the presence of RNF125. The level of RIG-I was reduced after addition of cycloheximide (CHX), when RNF125 was ectopically expressed, but no such reduction in RIG-I was observed in cells without ectopic expression of RNF125 (Fig. 2*g Upper*). Such degradation of RIG-I in cells treated with poly I:C was not observed in cells expressing RNF125 specific siRNA, siRNA125–3, although substantial amount of RIG-I degradation in cells treated with control siRNA could be observed (Fig. 2*g*).

E2 Enzymes Involved in Ubiquitin Conjugation to RIG-I. RNF125 interacts with several E2 enzymes (25), and one of these enzymes most likely acts as an E2 for ubiquitin conjugation to RIG-I. To identify the E2 acting upstream of RNF125 in RIG-I conjugation, we performed an *in vitro* assay examining ubiquitin conjugation to RIG-I [see supporting information (SI) Fig. 6]. We identified that UbcH1, UbcH5a, UbcH5b, and UbcH5c functioned as an E2 enzyme. The enzymes UbcH1 and UbcH5a-c conjugated ubiquitin to RNF125 and RIG-I via K48 (data not shown).

Further, by analyzing ubiquitin conjugation to RIG-I in 293FT cells by ectopic expression of the E2 enzymes, we observed only UbcH5c, and not other E2 enzymes, showing enhanced ubiquitin conjugation to RIG-I, suggesting that UbcH5c is the major E2 enzyme functioning *in vivo* (data not shown).

Expression of RNF125 Suppresses the Activation of IRF3. The ability of RNF125 to modulate RIG-I protein levels suggests that

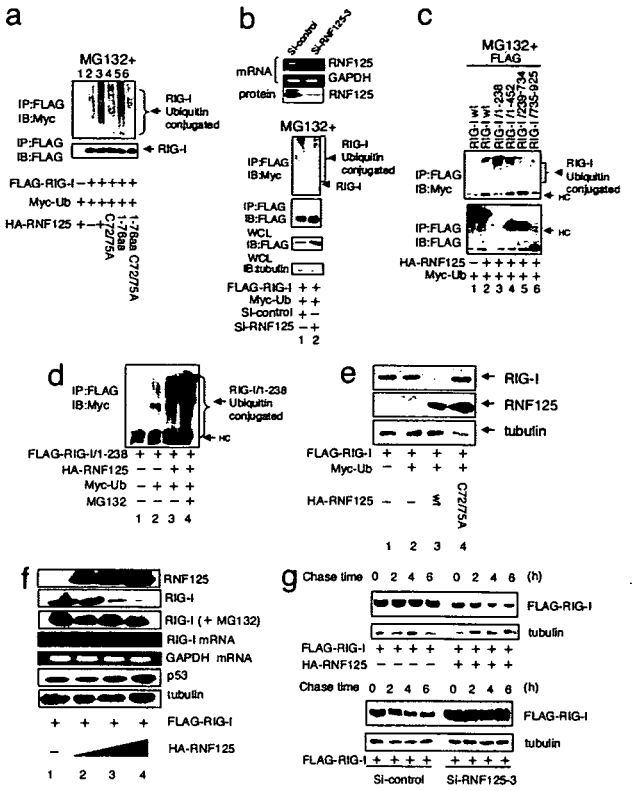

Fig. 2. Ubiquitin conjugation to RIG-I. (*a*) Ubiquitin conjugation to RIG-I by WT and mutant RNF125. Plasmids encoding FLAG-RIG-I and Myc-Ub were cotransfected into 292FT cells with a plasmid encoding either WT or mutant RNF125. The RIG-I ubiquitination was monitored by immunoprecipitation. All cells were treated with MG132. (*b*) Inhibition of RIG-I ubiquitin conjugation after suppression of endogenous RNF125. The siRNF125–3, an siRNA that down-regulates RNF125 mRNA, or a control siRNA were transfected into the 293FT cells. The mRNA and protein levels of RNF125 were monitored by RT-PCR or Western blot, respectively, 36 h after transfection (*Upper*). The 293FT cells transfected with plasmids encoding FLAG-RIG-I and Myc-Ub were simultaneously treated with control siRNA or siRNF125–3; RIG-I ubiquitination in cell lysates was then analyzed by coimmunoprecipitation. All cells were treated with MG132. The quantity of RIG-I present in the immunoprecipitants was monitored by immunoblot with an anti-FLAG antibody. The total RIG-I present in an aliquot of whole-cell lysate is also shown. Tubulin serves as the control in this analysis (*Lower*). (*c*) Analysis of the region for ubiquitin conjugation in RIG-I. Plasmids encoding HA-RNF125 and Myc-Ub were cotransfected into 293FT cells with WT or deletion mutants of FLAG-RIG-I. We analyzed cell lysates harvested 36 h after transfection for interactions between RNF125 and WT or mutant RIG-I by immunoprecipitation (note that the expression level of 1–238 was very low; despite the low levels, however, the interaction with RIG-I was clearly observed). All cells were treated with MG132. (*d*) Ubiquitin conjugation stimulates RIG-I degradation in a proteasome-dependent manner. Plasmids encoding a FLAG-tagged version of the RIG-I N terminus, FLAG-RIG-I/1–238, HA-RNF125, and Myc-Ub were transfected into 293FT cells as indicated. After culturing with or without MG132, the levels of ubiquitination were analyzed by immunoprecipitation. (*e*) RNF125 stimulates RIG-I degradation. Plasmids encoding FLAG-RIG-I and Myc-Ub were cotransfected into 293FT cells with WT or a point mutant of HA-RNF125. Cells were harvested 36 h after transfection and were analyzed for proteins by Western blot. (*f*) RIG-I was degraded by RNF125 in a dose-dependent manner. The 293FT cells were transfected with a plasmid encoding FLAG-RIG-I (0.5 μg) and varying doses of a plasmid encoding HA-RNF125 (0, 0.5, 1, and 2 μg). Half of each cell aliquot was treated with MG132. The levels of both RIG-I mRNA and protein were examined in cells harvested 48 h after transfection. "RIG-I (+MG132)" indicates analysis of the RIG-I protein in cells treated with MG132. As a control, the cellular proteins p53 and tubulin and GAPDH mRNA analyses are shown. (*g*) RIG-I was degraded by ectopic and endogenous RNF125. A plasmid encoding FLAG-RIG-I with or without a plasmid encoding HA-RNF125 was transfected into 293FT cells. Thirty-six hours after transfection, the cells were treated with CHX (final concentration, 50 μg/ml), and were analyzed by Western blot (*Upper*). Plasmids encoding FLAG-RIG-I and RNA for si-control or siRNF125–3 were transfected into 293FT cells. Twenty-four hours after transfection, these cells were treated with Poly I:C for 12 h, followed by addition of CHX. Cells were harvested at the indicated times after addition of CHX and analyzed by Western blot (*Lower*).

RNF125 may play an important role in the regulation of IRF3 activity. We analyzed this possibility by using a luciferase reporter gene driven by the IFNβ promoter, IFNβ-luc, to examine the effect of RNF125 on IRF3 activity after stimulation with poly I:C or Sendai virus infection (Fig. 3*a*). The 293FT cells expressing IFNβ-Luc, RIG-I, and RNF125 were treated with poly I:C or Sendai virus infection. We observed a marginal increase in luciferase activity in those cells lacking ectopic RIG-I and RNF125 expression (Fig. 3*a*, lanes 1–3). Luciferase activity was enhanced by the ectopic expression of RIG-I alone and further augmented by treatment with poly I:C or Sendai virus (Fig. 3*a*, lanes 4–6). Cells expressing RNF125, however, exhibited reduced reporter activity, and this decreased in a dose-dependent manner (Fig. 3*a*, lanes 7–15). The enhanced luciferase activity seen after polyIC treatment or Sendai virus infection was almost completely abrogated by high levels of RNF125 expression (Fig. 3*a*, lanes 12 and 15). Suppressive activity of IFNβ-luc was not observed by the mutant RNF125 that lacks the conjugation activity and ability to interact with RIG-I (Fig. 3*b*). Furthermore, we observed that ectopic RNF125 expression inhibited nuclear localization of IRF3 by poly I:C treatment (SI Fig. 7).

We next examined the effect of endogenous RNF125 on IRF3 activation by knocking down RNF125 mRNA by using siRNA. The 293FT cells treated with siRNF125–3 were subsequently transfected with plasmids encoding IFNβ-luc and RIG-I. Cells were then infected with Sendai virus or mock infected. Sendai virus-induced luciferase activity was substantially greater in cells in which RNF125 expression was suppressed by siRNF125–3 (Fig. 3*c Left*, lanes 2 and 4). Additionally, endogenous IFNβ mRNA production was also increased in those cells (Fig. 3*c Right*).

To examine whether the ability of RNF125 to suppress IRF3 activation in 293FT cells was physiologically relevant, an experiment was performed by using primary mouse embryonic fibroblasts (MEFs). RIG-I signaling is essential for virus-induced cytokine secretion in conventional dendritic cells (DCs) and MEFs (35). The MEFs transfected with plasmids encoding mouse RNF125 (mRNF125) and IFNβ-luc were infected with Sendai virus or mock infected. Induced induction of luciferase activity was directly correlated with the degree of Sendai virus infection (Fig. 3*d*). However, the induced luciferase activity was strongly suppressed by the ectopic expression of mRNF125 (Fig. 3*d*, lanes 7–9). Furthermore, transfection of MEFs with siRNF125–3 led to reduced mRNF125, mRNA, and protein levels (data not shown) and somewhat enhanced luciferase production after Sendai virus infection (Fig. 3*e*).

We further confirmed the suppression of RIG-I signaling by RNF125 by examining the release of IFNβ in the culture medium. In cells treated with poly I:C as well as infected with Sendai virus, IFNβ released was significantly reduced by the expression of RNF125 in a dose-dependent manner (Fig. 3*f*). Furthermore, MEFs treated with si-RNF125–3 showed substantial increase of IFNβ release in the culture medium upon polyI:C and Sendai virus infection (Fig. 3*g*).

RNF125, UbcH5, and RIG-I Are Up-Regulated by IFN-α and Poly I:C. The production of proteins related to Ubl conjugation is often regulated by IFNs (36). Thus, the modification of RIG-I by ubiquitin is most likely regulated by the coordinated induction of

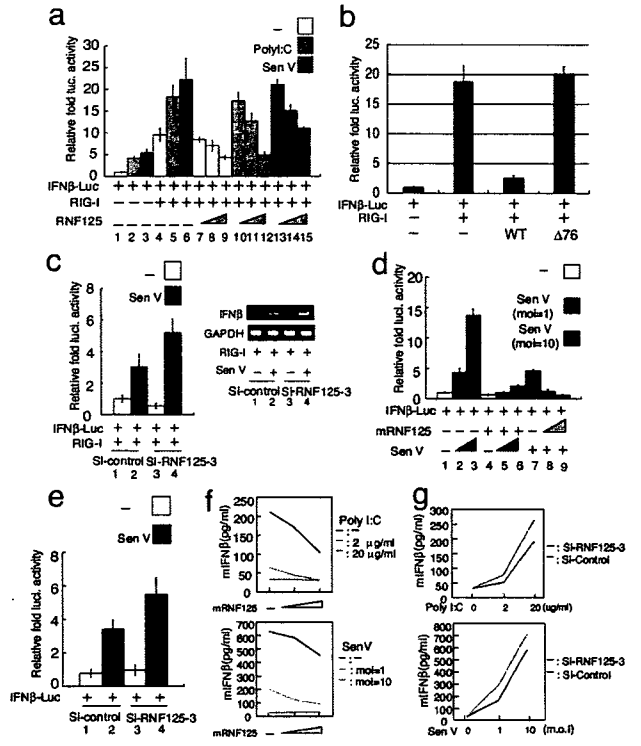

Fig. 3. Suppression of RIG-I function by ubiquitination. (*a*) The RNF125 suppressed the IFNβ-driven luciferase activity, activated by RIG-I (at the left). The 293FT cells were transfected with plasmids encoding RIG-I (50 ng) and IFNβ-luc (50 ng) with varying amounts of a plasmid encoding RNF125 (10, 50, and 100 ng). Twenty-four hours after transfection, cells were treated with polyIC (blue) or infected with Sendai virus (pink). Cells were harvested 12 h after the treatment; luciferase activity in the lysates was then measured. The RNF125 suppressed the production of IFNβ mRNA. (*b*) The 293FT cells transiently expressing IFNβ-luc, RIG-I, and RNF125WT or Δ76 were analyzed for luciferase activity 36 h after transfection. (*c*) Effect of siRNF125–3, a small inhibitory RNA specific for RNF125 mRNA, on IFNβ-luc activity and IFNβ level. The 293FT cells were transfected with plasmids encoding IFNβ-luc and RIG-I and treated with control siRNA or siRNF125–3. An aliquot of cells was then infected with Sendai virus. Twenty-four hours after infection, luciferase activity (*Left*) and IFNβ mRNA levels, assessed by RT-PCR (*Right*), were measured. (*d*) Effect of mouse RNF125 on endogenous RIG-I signaling in primary MEFs. The MEFs were transfected with plasmids encoding mouse RNF125 (100 ng in lanes 4, 5, 6, and 8 or 200 ng in lane 9) and IFNβ-luc (50 ng) in combination as indicated. Twelve hours after transfection, cells were infected with Sendai virus at the indicated multiplicity of infection (MOI) or mock infected. Luciferase activity in cell lysates prepared 24 h after treatment was measured. White box, mock infected; pink box, Sendai virus infected with MOI 1; black box, Sendai virus with MOI of 10. (*e*) The MEFs were transfected with plasmids encoding IFNβ-luc and treated with control siRNA or siRNF125–3 (final concentration of 8 nM). Cells were then infected with Sendai virus at MOI of 1. Twenty-four hours after infection, luciferase activity was measured. (*f*) The level of IFNβ in culture medium in cells was decreased in an RNF125 dose-dependent manner. Cells transfected with different amounts of plasmids encoding RNF125 were treated with 0 (green), 2 (pink), and 20 (blue) μg/ml of poly I:C (*Upper*) and with 0 (green), 1 (pink), and 10 MOI (blue) of Sendai virus (*Upper*). Twelve hours after the treatment, IFNβ in the culture medium was measured by ELISA system. (*g*) The level of IFNβ was increased in MEFs treated with siRNA for RNF125-specific mRNA. Cells treated with control siRNA (black bars) or siRNA125–3 (pink bars) were treated with different doses of poly I:C or Sendai virus infection and were analyzed for IFNβ in culture medium.

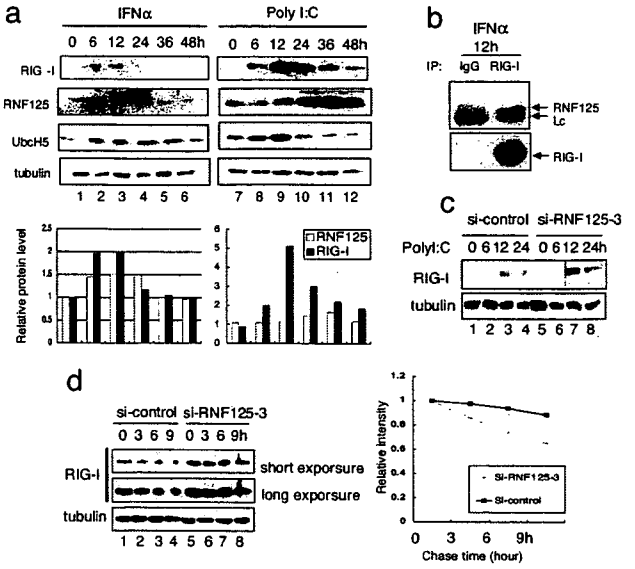

Fig. 4. Induction of RIG-I and the Ubls by IFNα or poly I:C treatment. (*a*) HepG2 cells were harvested at the indicated times after treatment with IFNα (10^3 units/ml) or Poly I:C (2 μg/ml) and were analyzed for protein levels by Western blot. As a control, the level of tubulin is shown. The protein level of each band is quantified and graphed. (*b*) Endogenous association of RIG-I and RNF125. Jurkat cells were incubated with IFNα (1,000 units/ml) and MG132 (final 10 μM). After 12 h, whole-cell lysates were subjected to immunoprecipitation assay using anti-RIG-I antibody or control antibody, followed by immunoblotting for detection of RNF125 and RIG-I. (*c*) Influence of siRNA specific to RNF125 for RIG-I levels. Cells treated with siRNA were further treated with poly I:C and then harvested at the indicated times after poly I:C treatment. The lysates were analyzed for the levels of endogenous RIG-I. Tubulin acts as a control. (*d*) HepG2 cells treated with siRNA were further treated with IFNα for 12 h and then harvested at the indicated times after CHX treatment. The lysates were analyzed for the levels of endogenous RIG-I. Tubulin acts as a control. The intensity of each band is quantified and graphed.

Ubl-conjugating proteins. We analyzed the levels of RIG-I, RNF125, and UbcH5 in HepG2 cells at various times after treatment with IFNα and poly I:C (Fig. 4a). Low levels of RNF125 were present before IFNα and Poly I:C treatment, but its expression peaked 12–36 h after induction. Although RIG-I was barely detectable at the time of induction, it became detectable at 6 h and peaked at 12 h. The decreases in RIG-I expression correlated temporally with the increases in RNF125 and UbcH5 (Fig. 4*a*), suggesting that RNF125 decreased the levels of RIG-I after IFN induction. Quantitative analysis indicated that RIG-I level showed reverse correlation of RNF125 (Fig. 4*a*, graph). The fact that constitutive association of endogenous RIG-I and RNF125 (Fig. 4*b*) supports the possibility that RNF125 conjugates ubiquitin to RIG-I to promote proteasomal degradation. We confirmed this hypothesis by treating cells with RNF125 siRNA. In cells treated with control siRNA, RIG-I expression increased at 12 and 24 h after poly I:C treatment, but, in cells treated with siRNF125–3, RIG-I expression was higher, and it sustained longer than treated control cells (Fig. 4*c*, compare lanes 3 and 7 and 4 and 8). To measure a half-life of RIG-I, we treated HepG2 cells expressing siRNA specific to RNF125 or control siRNA with IFNα for 12 h and then added CHX. Cells harvested at the indicated time after CHX treatment were analyzed for RIG-I by Western blot and quantified the intensity of the bands (Fig. 4*d*). Calculated half-life of RIG-I in cells treated with siRNA specific to RNF125 was 16 h and 8 h in cells treated with control siRNA.

RNF125 Exhibits Ubiquitin-Conjugating E3-Ligase Activity for MDA5 and IPS1. MDA5 is a member of the RIG-I protein family and contains CARD domain. The IPS1, a CARD-containing protein, downstream of RIG-I signaling interacts with RIG-I